The E3 Ubiquitin Ligases TRIM17 and TRIM41 Modulate α-Synuclein Expression by Regulating ZSCAN21

Irena Lassot, Stéphan Mora, Suzanne Lesage, Barbara A Zieba, Emmanuelle Coque, Christel Condroyer, Jozef Piotr Bossowski, Barbara Mojsa, Cécilia Marelli, Caroline Soulet, et al.

Article

Cell Reports

The E3 Ubiquitin Ligases TRIM17 and TRIM41 Modulate α-Synuclein Expression by Regulating ZSCAN21

Graphical Abstract

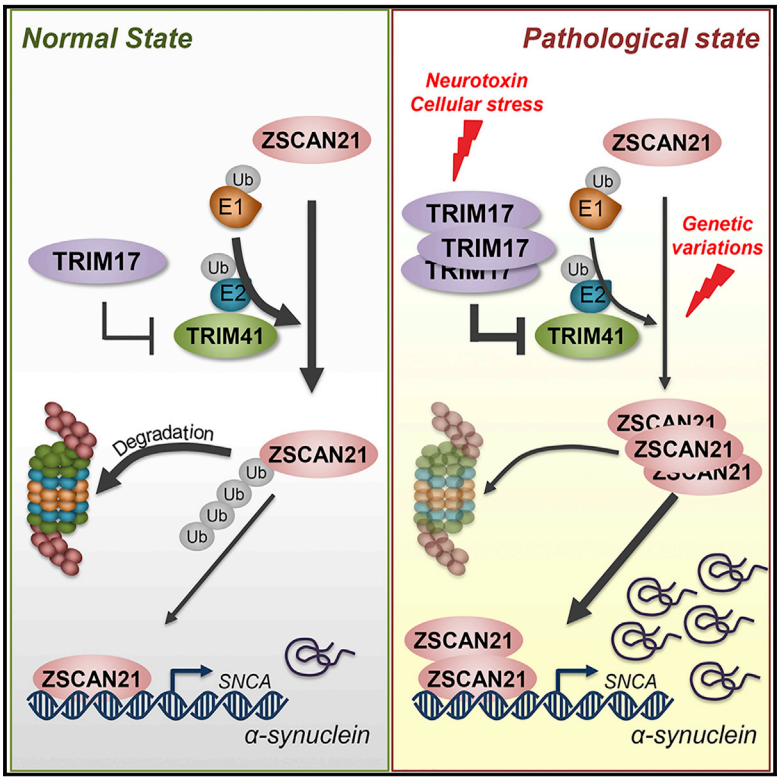

Highlights

- The transcription factor ZSCAN21 induces α-synuclein expression in neuronal cells
- TRIM41 ubiquitinates ZSCAN21 and TRIM17 inhibits its activity
- Variants of *TRIM41* and *ZSCAN21* in patients with familial PD co-segregate with PD
- These genetic variations result in stabilization of the ZSCAN21 protein

Authors

Iréna Lassot, Stéphan Mora, Suzanne Lesage, ..., Miquel Vila, Alexis Brice, Solange Desagher

Correspondence

irena.lassot@igmm.cnrs.fr

In Brief

Although α-synuclein expression plays a crucial role in Parkinson disease (PD), its transcriptional regulation is largely unknown. Lassot et al. describe a pathway regulating α-synuclein expression. Identification and characterization of genetic variations in patients suggest that deregulation of this pathway may be involved in the pathogenesis of PD.

Lassot et al., 2018, Cell Reports *25*, 2484–2496
November 27, 2018
https://doi.org/10.1016/j.celrep.2018.11.002

CellPress

OPEN ACCESS
CellPress

Cell Reports
Article

The E3 Ubiquitin Ligases TRIM17 and TRIM41 Modulate α-Synuclein Expression by Regulating ZSCAN21

Iréna Lassot,[1,9,*] Stéphan Mora,[1] Suzanne Lesage,[2,3] Barbara A. Zieba,[1] Emmanuelle Coque,[1] Christel Condroyer,[2,3] Jozef Piotr Bossowski,[1] Barbara Mojsa,[1,7] Cecilia Marelli,[1,8] Caroline Soulet,[1] Christelle Tesson,[2,3] Iria Carballo-Carbajal,[4] Ariadna Laguna,[4] Graziella Mangone,[2,3] Miquel Vila,[4,5,6] Alexis Brice,[2,3] and Solange Desagher[1]

[1]Institut de Génétique Moléculaire de Montpellier, University of Montpellier, CNRS, Montpellier, France
[2]Sorbonne Universités, UPMC Université de Paris 06, UMR S 1127, Institut du Cerveau et de la Moelle épinière (ICM), Paris, France
[3]INSERM U 1127, CNRS UMR 7225, AP-HP, Pitié-Salpêtrière Hospital, Paris, France
[4]Neurodegenerative Diseases Research Group, Vall d'Hebron Research Institute (VHIR)-Center for Networked Biomedical Research on Neurodegenerative Diseases (CIBERNED), 08035 Barcelona, Spain
[5]Department of Biochemistry and Molecular Biology, Autonomous University of Barcelona, 08193 Barcelona, Spain
[6]Catalan Institution for Research and Advanced Studies (ICREA), 08010 Barcelona, Spain
[7]Present address: Centre for Gene Regulation and Expression, Sir James Black Centre, School of Life Sciences, University of Dundee, Dundee DD1 5EH, UK
[8]Present address: Department of Neurology, University Hospital Gui de Chauliac, Montpellier, France
[9]Lead Contact
*Correspondence: irena.lassot@igmm.cnrs.fr
https://doi.org/10.1016/j.celrep.2018.11.002

SUMMARY

Although accumulating data indicate that increased α-synuclein expression is crucial for Parkinson disease (PD), mechanisms regulating the transcription of its gene, *SNCA*, are largely unknown. Here, we describe a pathway regulating α-synuclein expression. Our data show that ZSCAN21 stimulates *SNCA* transcription in neuronal cells and that TRIM41 is an E3 ubiquitin ligase for ZSCAN21. In contrast, TRIM17 decreases the TRIM41-mediated degradation of ZSCAN21. Silencing of *ZSCAN21* and *TRIM17* consistently reduces *SNCA* expression, whereas *TRIM41* knockdown increases it. The mRNA levels of *TRIM17*, *ZSCAN21*, and *SNCA* are simultaneously increased in the midbrains of mice following MPTP treatment. In addition, rare genetic variants in *ZSCAN21*, *TRIM17*, and *TRIM41* genes occur in patients with familial forms of PD. Expression of variants in *ZSCAN21* and *TRIM41* genes results in the stabilization of the ZSCAN21 protein. Our data thus suggest that deregulation of the TRIM17/TRIM41/ZSCAN21 pathway may be involved in the pathogenesis of PD.

INTRODUCTION

Parkinson disease (PD) is one of the most common neurodegenerative disorders. Although most cases of PD are sporadic, >10% are associated with mutations in genes with autosomal dominant or recessive inheritance. The first gene found to be mutated in familial PD is *SNCA*, which encodes α-synuclein, an abundant presynaptic protein. *SNCA* is arguably the most important gene linked to PD (Corti et al., 2011; Dehay et al., 2015). Notably, many studies suggest that even a moderate increase in wild-type (WT) α-synuclein is enough to cause both inherited and sporadic forms of PD (Devine et al., 2011; Stefanis, 2012). Duplications or triplications of the WT *SNCA* locus give rise to dominantly inherited PD, the severity of the disease being directly correlated with α-synuclein mRNA and protein levels (Chartier-Harlin et al., 2004; Farrer et al., 2004; Miller et al., 2004). Genetic variability in the promoter region of *SNCA* associated with increased risk for PD has also been correlated with the upregulation of α-synuclein expression (Cronin et al., 2009; Linnertz et al., 2009). Although still under debate, the mRNA levels of α-synuclein seem to be increased in the *substantia nigra* of sporadic PD patients compared to that of controls (Gründemann et al., 2008). Finally, overexpression of WT α-synuclein leads to phenotypes resembling PD in animal models (Masliah et al., 2000; Nuber et al., 2013; Yamada et al., 2004).

Nevertheless, *SNCA* transcriptional regulation has been poorly studied, and only a few transcription factors have been described for this gene up to now (Clough et al., 2009; Dermentzaki et al., 2016; Scherzer et al., 2008; Wright et al., 2013). Independent studies have shown that elements within intron 1 of *SNCA* are involved in its transcriptional regulation (Brenner et al., 2015; Clough and Stefanis, 2007; Dermentzaki et al., 2016; Duplan et al., 2016; Jowaed et al., 2010; Scherzer et al., 2008). Among the transcription factors that can target this region, ZSCAN21 (also known as Zipro1/RU49/ZNF38) seems to play an important role (Brenner et al., 2015; Clough et al., 2009; Dermentzaki et al., 2016). Initially identified as a marker for the granule neuron lineage in the CNS (Yang et al., 1996), ZSCAN21 seems to be expressed throughout the brain, in humans and mice, at different levels, depending on the structure (Dermentzaki et al., 2016; Sunkin et al., 2013).

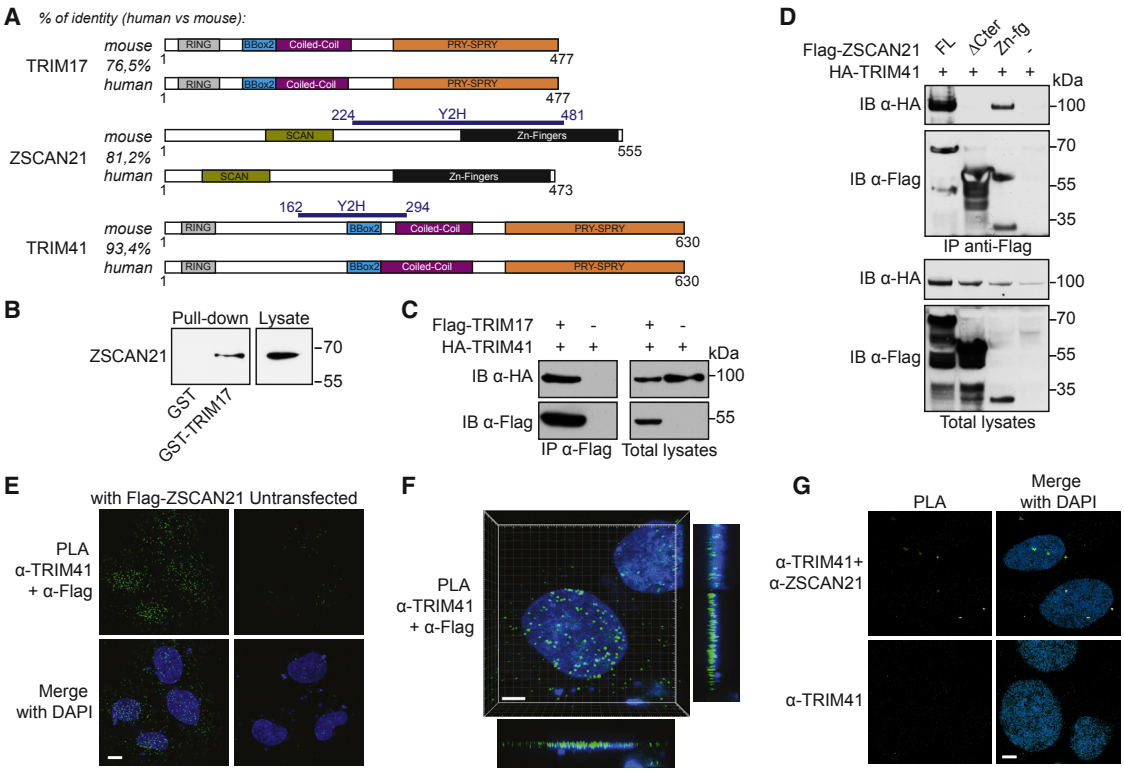

Figure 1. ZSCAN21 Interacts with Both TRIM17 and TRIM41

(A) Schematic representations of human and mouse TRIM17, ZSCAN21, and TRIM41 structures. The different protein-protein and protein-DNA interaction domains are indicated. The smallest cDNA clones of ZSCAN21 and TRIM41 isolated in the yeast two-hybrid (Y2H) screen are indicated.

(B) Purified recombinant GST and GST-TRIM17 were incubated with a lysate from mouse cerebellar granule neurons that had been cultured in low potassium medium to induce apoptosis. Endogenous mouse ZSCAN21 precipitated by glutathione beads was visualized by western blot using anti-ZSCAN21 antibody.

(C and D) 293T cells were co-transfected with HA-TRIM41 and either FLAG-TRIM17 or an empty plasmid in (C), or with mouse FLAG-ZSCAN21 (FL), FLAG-ZSCAN21ΔCter (deleted from amino acids [aas] 357–555), the zinc fingers domain of ZSCAN21 fused to the FLAG tag (Zn-fg, aas 359–555), or an empty plasmid (–) in (D), for 24 hr. FLAG-fusion proteins were immunoprecipitated using anti-FLAG antibody. Immunoprecipitates (IPs) and cell lysates were analyzed by western blot (IB) using indicated antibodies.

(E) Interaction between transfected FLAG-ZSCAN21 and endogenous TRIM41 was estimated by proximity ligation assay using anti-FLAG and anti-TRIM41 antibodies in U2OS cells. Bright spots are detected when the two proteins are in close proximity (left). Negative control (right) was obtained using untransfected cells. Cells were analyzed by confocal microscopy. Scale bar, 10 μm.

(F) Three-dimensional (3D) images of U2OS cells shown in (E) obtained from z series in confocal microscopy with two lateral views. Scale bar, 5 μm.

(G) Interaction between endogenous ZSCAN21 and endogenous TRIM41 proteins was estimated by proximity ligation assay using anti-ZSCAN21 and anti-TRIM41 antibodies in SH-SY5Y cells. Bright spots are detected when the two proteins are in close proximity (top). Negative control (bottom) was obtained using only anti-TRIM41 antibody. Cells were analyzed by confocal microscopy. Scale bar, 5 μm.

See also Figure S1.

In previous studies, we have shown that mouse TRIM17 initiates neuronal apoptosis (Lassot et al., 2010), notably by contributing to the ubiquitination and degradation of the anti-apoptotic protein Mcl-1 (Magiera et al., 2013). TRIM17 is a member of the TRIM protein family, which constitutes the largest subclass of "single protein RING finger" E3 ubiquitin ligases (Kimura et al., 2016; Meroni and Diez-Roux, 2005). Identification of ZSCAN21 and TRIM41 as binding partners of TRIM17 prompted us to examine the role of the TRIM17 and TRIM41 E3 ubiquitin ligases in the stability of ZSCAN21 and hence in the transcriptional regulation of *SNCA*. Our results suggest that TRIM17 stabilizes ZSCAN21 by inhibiting TRIM41 and thus favors α-synuclein expression. Our silencing data in SH-SY5Y cells and expression data in a 1-methyl-4-phenyl-1,2,3,6-tetrahydropyridine (MPTP)-based animal model of PD support this hypothesis. Moreover, we identified rare genetic variants in *ZSCAN21*, *TRIM17*, and *TRIM41* genes in patients with familial PD. Expression of two of these variants resulted in ZSCAN21 stabilization and increased apoptosis, suggesting a possible pathogenic effect.

RESULTS

TRIM17 Interacts with Both ZSCAN21 and TRIM41

We identified ZSCAN21 and TRIM41 as putative binding partners of TRIM17 in a yeast two-hybrid (Y2H) screen (Mojsa et al., 2015) (Figure 1A). We first confirmed the interaction between recombinant mouse glutathione S-transferase (GST)-TRIM17 and endogenous mouse ZSCAN21 in a cell extract

from apoptotic cerebellar granule neurons, using a GST-pull-down assay (Figure 1B). Co-immunoprecipitation experiments showed that the human forms of ZSCAN21 and TRIM17 also bind to each other when co-expressed in 293T cells (Figure S1A) and that TRIM17 binds to TRIM41 (Figure 1C). As TRIM17 interacts with both ZSCAN21 and TRIM41, we tested whether ZSCAN21 interacts also with TRIM41. We found that hemagglutinin (HA)-TRIM41 co-immunoprecipitated with FLAG-ZSCAN21 (Figure 1D). Moreover, using an *in situ* proximity ligation assay (PLA), we detected an interaction between endogenous TRIM41 and FLAG-ZSCAN21 in U2OS cells (Figures 1E and 1F) and between endogenous TRIM41 and ZSCAN21 proteins in SH-SY5Y cells (Figure 1G). This interaction took place mainly in the nucleus, although it also occurred in the cytoplasm (Figures 1E–1G). Among other TRIM proteins, ZSCAN21 appeared to bind specifically to TRIM17 and TRIM41 (Figures S1C and S1D).

Deletion of the N-terminal end of ZSCAN21 did not affect its interaction with TRIM17 (Figure S1A), but it did slightly decrease its interaction with TRIM41 (Figures 1D and S1B) in co-immunoprecipitation experiments. In contrast, deletion of the C-terminal part of ZSCAN21, containing seven zinc fingers, abrogated its interaction with TRIM17 (Figure S1A) and with TRIM41 (Figures 1D and S1B). Furthermore, a construction expressing only the zinc finger domain of ZSCAN21 was sufficient to co-immunoprecipitate TRIM41 (Figure 1D). These data indicate that ZSCAN21 interacts with both TRIM17 and TRIM41 through its zinc finger domain.

TRIM41 Is an E3 Ubiquitin Ligase for ZSCAN21

Because TRIM17 and TRIM41 are E3 ubiquitin ligases (Chen et al., 2007; Lassot et al., 2010), we examined whether they could mediate ZSCAN21 ubiquitination. The ubiquitination level of ZSCAN21 was greatly increased by TRIM41 but not by TRIM17, nor TRIM39 and TRIM44, two other TRIM proteins that interact with TRIM17 (Rual et al., 2005; Urano et al., 2009; Woodsmith et al., 2012) (Figure 2A). In addition, the inactive deletion mutant TRIM41-ΔRING did not promote ZSCAN21 ubiquitination, in contrast to WT TRIM41 (Figure 2B), confirming that the RING domain of TRIM41 that is responsible for its E3 ubiquitin ligase activity is directly involved in ZSCAN21 ubiquitination.

Because ubiquitination often targets proteins for proteasomal degradation, we analyzed ZSCAN21 protein levels following proteasome inhibition using MG132. ZSCAN21 was increased to a similar extent as the short-lived protein MCL-1, suggesting that ZSCAN21 is also a proteasomal substrate (Figure 2C). Moreover, co-transfection of increasing amounts of TRIM41 decreased the ZSCAN21 level (Figure 2D). To determine whether this was due to an increase in ZSCAN21 degradation, we measured the half-life of ZSCAN21 in SH-SY5Y neuroblastoma cells transfected with different TRIM proteins. Consistent with our ubiquitination data, the stability of ZSCAN21 was not affected by the presence of TRIM17, TRIM39, or TRIM44 (Figures 2E and 2F). In contrast, ZSCAN21 was strongly destabilized in the presence of TRIM41 (Figures 2E and 2F). The half-life of ZSCAN21 was consistently strongly increased following the silencing of TRIM41 using specific small interfering RNAs (siRNAs) (Figures 2G, S2A, and S2B). These results indicate that TRIM41 acts as an E3 ubiquitin ligase of ZSCAN21, thereby promoting its degradation.

ZSCAN21 Favors *SNCA* Transcription

ZSCAN21 has been shown to promote transcription of the *SNCA* gene in PC12 cells and in rat primary cortical neurons (Clough et al., 2009). One conserved consensus-binding element for ZSCAN21, AGTAC (Yang et al., 1996), was consistently identified in the 5′-region of intron 1 of *SNCA* (Clough et al., 2009) (Figure 3A). To better characterize ZSCAN21 activity on *SNCA*, we first performed an oligonucleotide pull-down assay using biotinylated 27-mer oligonucleotides corresponding to the region of *SNCA* harboring the ZSCAN21 binding site. The WT sequence precipitated endogenous ZSCAN21 from Neuro2A cell lysates, whereas a mutated sequence in which the AGTAC motif was replaced by AAAAA could not (Figure 3B, top). This binding was decreased by increasing amounts of competing non-biotinylated oligonucleotide (Figure 3B, top) and was specific for ZSCAN21. The unrelated c-Jun transcription factor only weakly interacted with the WT or the mutated oligonucleotides (Figure 3B, bottom). The WT form and the N-terminal deletion mutant (ΔNter) of ZSCAN21, both containing the zinc fingers domain, were also precipitated by the oligonucleotide from the total lysate of transfected SH-SY5Y cells, whereas the C-terminal deletion mutant (ΔCter) of ZSCAN21 was not (Figure 3C). Furthermore, we performed chromatin immunoprecipitation (ChIP) experiments in SH-SY5Y cells transfected with WT FLAG-ZSCAN21 using an anti-FLAG antibody and primers flanking the region of intron 1 containing the consensus-binding site for ZSCAN21 in the *SNCA* gene. In all of the experiments, we detected an enrichment of the consensus-binding sequence in the FLAG-ZSCAN21 ChIP compared to the negative control, suggesting a specific ZSCAN21 binding on this consensus sequence (Table S1).

To test the effect of ZSCAN21 on *SNCA* expression, SH-SY5Y cells were transfected with ZSCAN21, its partner TRIM17, or its E3 ubiquitin ligase TRIM41, together with GFP. Transfected cells were sorted using flow cytometry, and their content of endogenous *SNCA* mRNA was assessed by real-time PCR. Transfection of ZSCAN21 induced a low but statistically significant increase in the *SNCA* mRNA level, whereas TRIM41 decreased it (Figure 3D). We were surprised to find that TRIM17 increased the *SNCA* mRNA level to an extent similar to ZSCAN21 (Figure 3D). These effects were associated with consistent changes in the protein level of α-synuclein. Immunostaining of α-synuclein was significantly increased in individual SH-SY5Y cells transfected with ZSCAN21 or TRIM17 and significantly decreased following TRIM41 transfection, compared to the negative control ZSCAN21ΔCter (Figures 3E–3I). In these experiments, immunofluorescence intensity was assessed only in healthy cells to avoid any bias due to cell shrinkage resulting from apoptosis, except for TRIM17 overexpression, which we reported to be pro-apoptotic (Lassot et al., 2010). In this case, both healthy and apoptotic cells were taken into account, and a part of the increased immunofluorescence may be secondary to cell shrinkage (Figures 3E and 3H). Nevertheless, these experiments suggest that binding of ZSCAN21 to its consensus motif in the *SNCA* locus stimulates the transcription of the gene.

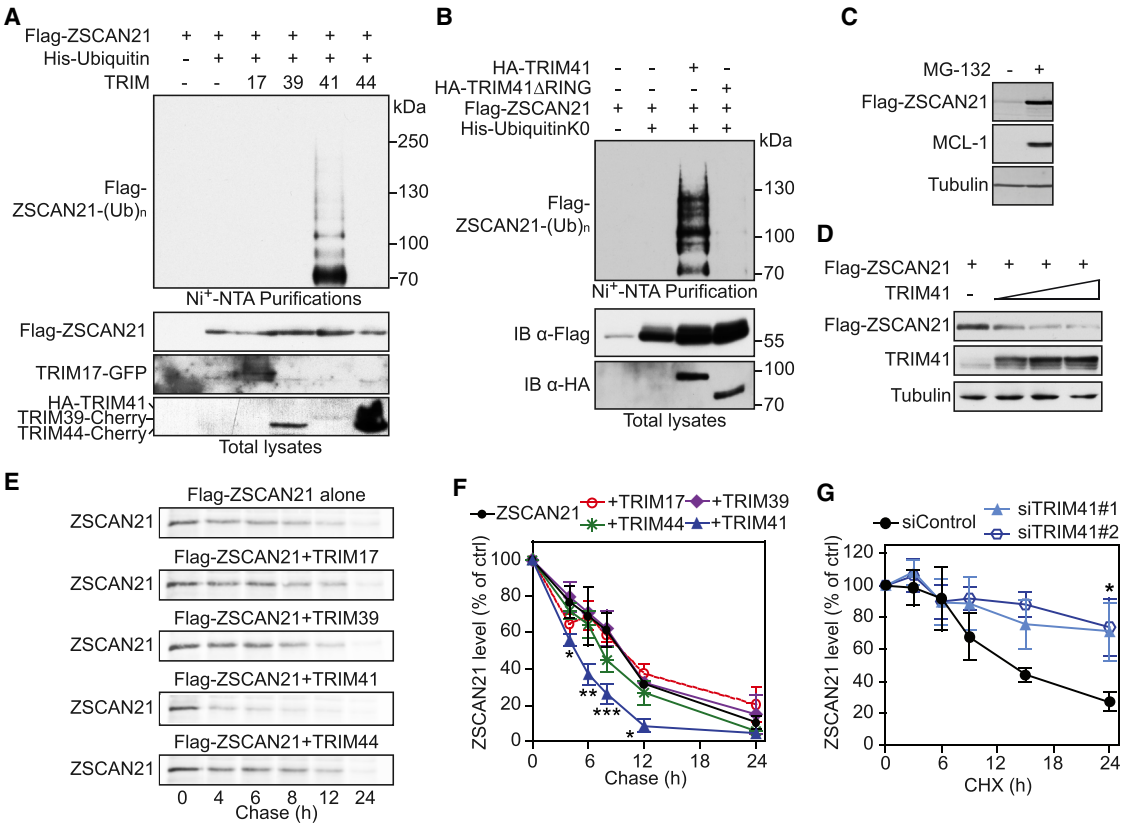

Figure 2. TRIM41, but Not TRIM17, Is an E3 Ubiquitin Ligase for ZSCAN21

(A) 293T cells were transfected with FLAG-ZSCAN21 in the presence or absence of His-ubiquitin together with TRIM17-GFP, TRIM39-mCherry, HA-TRIM41, or TRIM44-mCherry for 24 hr. Then, cells were incubated for 6 hr with 20 μM MG-132. The ubiquitinated proteins were purified and analyzed by western blot using anti-FLAG antibodies. In a separate SDS-PAGE, the input lysates used for the purification were analyzed with different antibodies, as indicated.

(B) 293T cells were transfected with FLAG-ZSCAN21 in the presence or absence of His-ubiquitinK0 and HA-TRIM41 or HA-TRIM41ΔRING for 24 hr. Then, cells were treated as in (A). UbiquitinK0 mutant, which is not able to form poly-ubiquitin chains, was used to better see differences in the ubiquitination rate.

(C) 293T cells were transfected with FLAG-ZSCAN21 for 24 hr and then treated or not with 10 μM MG-132 for 16 hr. Cell lysates were analyzed by western blot using anti-FLAG, anti-MCL-1, and anti-tubulin antibodies.

(D) 293T cells were co-transfected with FLAG-ZSCAN21 and increasing amounts of TRIM41 for 24 hr. Cell lysates were analyzed by western blot using anti-FLAG, anti-TRIM41, and anti-tubulin antibodies.

(E) SH-SY5Y cells were transfected with FLAG-ZSCAN21 in the presence or the absence of TRIM17-GFP, TRIM39-mCherry, HA-TRIM41, or TRIM44-mCherry for 24 hr. Then, cells were metabolically labeled with [^{35}S]-Met for 1 hr (pulse) and harvested at the indicated times after washing and incubation in cold culture medium (chase). FLAG-ZSCAN21 was then immunoprecipitated using anti-FLAG beads, separated by SDS-PAGE, and visualized by autoradiography [^{35}S].

(F) The intensity of the bands on the autoradiograms of four independent experiments performed as in (E) was quantified. *$p < 0.05$, **$p = 0.0012$, ***$p = 0.0004$, significantly different from ZSCAN21 alone at the given time points.

(G) SH-SY5Y cells were transfected with FLAG-ZSCAN21 together with two distinct siRNA directed against TRIM41 and a negative control siRNA. Then, cells were treated with 10 μg/mL cycloheximide for increasing times. Cell lysates were analyzed by western blot. The intensity of the ZSCAN21 bands was quantified and normalized with actin. *$p < 0.05$, significantly different from siControl ($n = 3$).

See also Figure S2.

TRIM17 Inhibits TRIM41-Mediated ZSCAN21 Ubiquitination

As overexpression of TRIM17 increased α-synuclein expression (Figures 3D, 3E, and 3H), we examined the effect of TRIM17 on TRIM41-mediated ubiquitination of ZSCAN21. Overexpression of TRIM17 totally abolished the increase in ZSCAN21 ubiquitination induced by TRIM41 (Figure 4A). The inactive RING mutant of TRIM17 (TRIM17 p.C16A [Lassot et al., 2010]) had the same effect as WT TRIM17, suggesting that the RING domain and thus the E3 ubiquitin ligase activity of TRIM17 are not required for its inhibitory effect (Figure S3A). Accordingly, the protein level of ZSCAN21 progressively increased when co-transfected with increasing amounts of TRIM17 and a fixed amount of TRIM41 (Figure S3B), and it progressively decreased with increasing amounts of TRIM41 and a fixed amount of TRIM17 (Figure S3B). Overexpression of TRIM17 completely prevented the destabilization of ZSCAN21 induced by TRIM41 (Figure 4B). Moreover, silencing of TRIM17 induced a significant decrease in the endogenous ZSCAN21 protein level in SH-SY5Y cells following protein synthesis inhibition by cycloheximide (Figures 4C–4E, S3C, and S3D). In contrast, silencing of TRIM41 significantly increased the endogenous ZSCAN21 protein level in these conditions

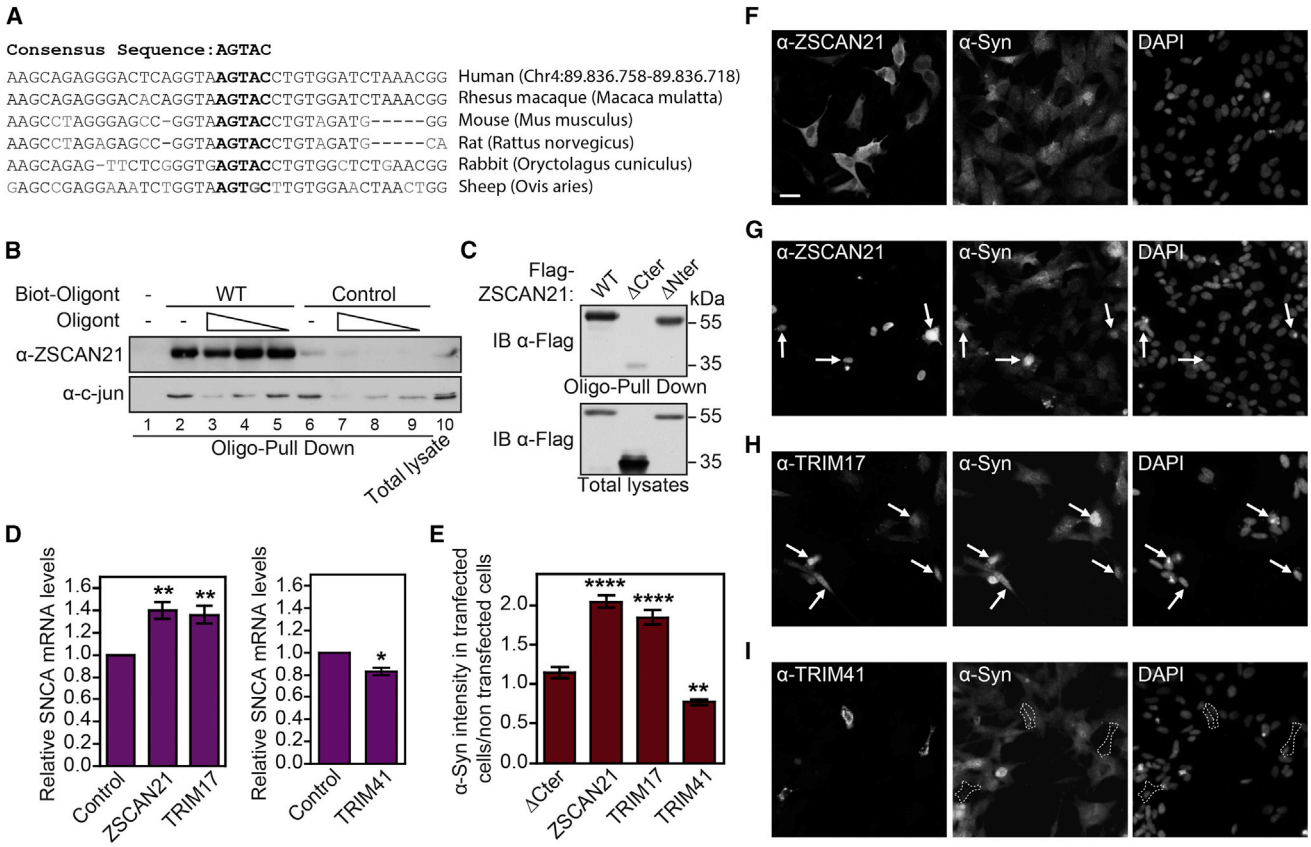

Figure 3. ZSCAN21 Favors the Transcription of *SNCA*

(A) Genomic location of the highly conserved binding motif for ZSCAN21 in the human *SNCA* locus and sequence alignment with various species. Conserved nucleotides in consensus binding sites (bold) and nucleotides varying from the human sequence (gray).

(B) Lysates from Neuro2A cells were incubated with a biotinylated oligonucleotide containing either the wild-type (WT) consensus-sequence binding element of *SNCA* intron 1 or a mutated sequence (control) in the presence or absence of increasing amounts of non-biotinylated WT oligonucleotide. The initial total lysate and oligonucleotide pull-down precipitates were analyzed by western blot using anti-ZSCAN21 and anti-c-Jun antibodies.

(C) SH-SY5Y cells were transfected with different forms of FLAG-ZSCAN21 for 24 hr. Cell lysates were subjected to oligonucleotide pull-down with the WT oligonucleotide, as in (B).

(D) SH-SY5Y cells were transfected with ZSCAN21 or TRIM17 (left), or TRIM41 (right), or empty plasmid (control), together with GFP. Transfected cells were sorted by flow cytometry, and their *SNCA* mRNA content was measured by real-time qPCR. Left: **$p < 0.005$ ($n = 5$); right: *$p = 0.0174$ ($n = 4$; paired t test), significantly different from control.

(E) SH-SY5Y cells were transfected with WT FLAG-ZSCAN21, FLAG-ZSCAN21ΔCter, HA-TRIM17, or HA-TRIM41 for 24 hr. Cells were analyzed by immunofluorescence using antibodies against ZSCAN21, TRIM17, or TRIM41, together with anti-α-synuclein antibody. Intensity of α-synuclein immunofluorescence was analyzed with Cell Profiler software in each cell. The graph represents the ratio between α-synuclein intensity in ~100 transfected cells compared to the average of α-synuclein intensity of ~100 non-transfected cells. Only living cells were taken into account, except for TRIM17 overexpression, which was pro-apoptotic, as previously reported (Lassot et al., 2010). **$p = 0.0083$, ****$p = 0.0001$, significantly different from ΔCter used as a negative control.

(F–I) Representative pictures used in (E). SH-SY5Y cells were transfected with Flag-ZSCAN21ΔCter (F), WT Flag-ZSCAN21 (G), HA-TRIM17 (H), or HA-TRIM41 (I). Arrows or dotted lines indicate transfected cells. Scale bar, 30 μm.

See also Table S1.

(Figures 4C–4E, S3C, and S3D), suggesting that endogenous TRIM17 stabilizes, whereas endogenous TRIM41 destabilizes, endogenous ZSCAN21. These results indicate that TRIM17 inhibits the ubiquitination and degradation of ZSCAN21 induced by TRIM41.

We next investigated the mechanism underlying this inhibitory effect of TRIM17. First, *in vitro* auto-ubiquitination of TRIM41 was strongly decreased in the presence of TRIM17, suggesting that TRIM17 inhibits the E3 ubiquitin ligase activity of TRIM41 (Figure 4F). The ubiquitination of TRIM41 was also totally abolished when co-transfected with TRIM17 in cells (Figure S3E). Then, we examined the binding preference of the three partners by a series of co-immunoprecipitation experiments (Figures S3F–S3H). These data suggest that TRIM17 and TRIM41 form preferentially homotypic rather than heterotypic interactions, as suggested by others (Woodsmith et al., 2012), and thus bind more easily to each other than to ZSCAN21. The interaction of TRIM41 with ZSCAN21 was significantly decreased in the presence of TRIM17. The amount of TRIM41 co-immunoprecipitated with ZSCAN21 was 0.32 ± 0.20 ($p = 0.004$, unpaired t test,

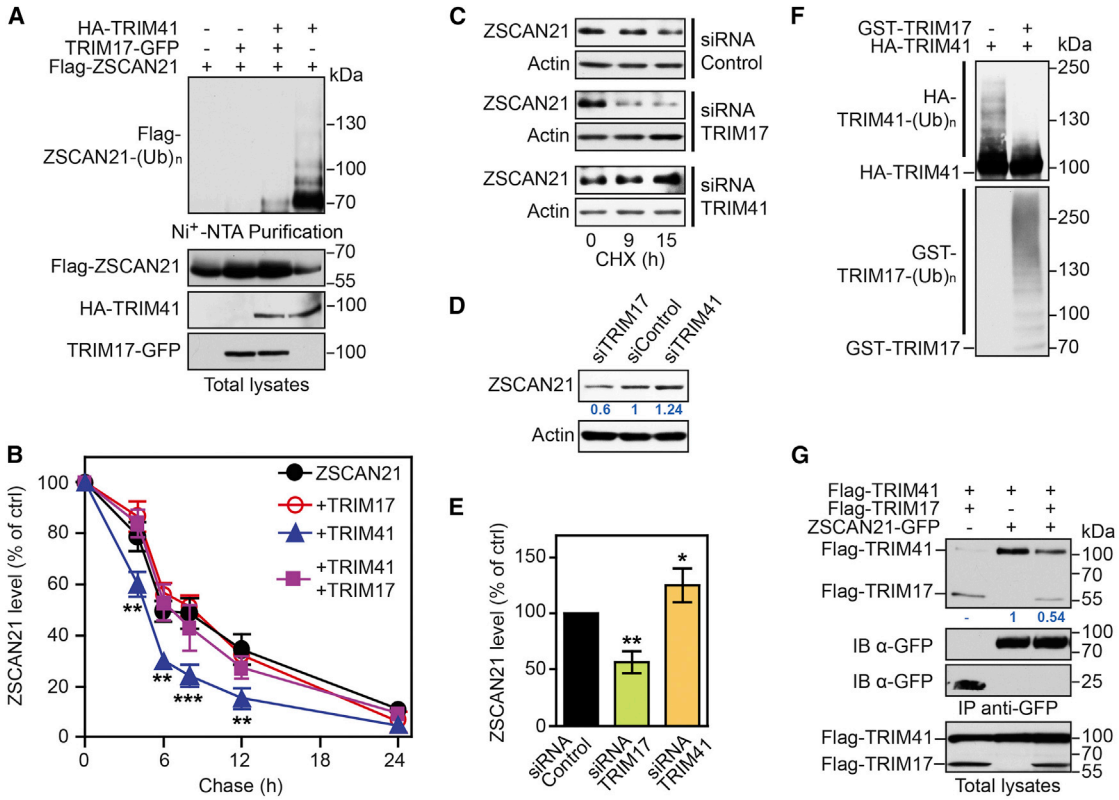

Figure 4. TRIM17 Inhibits TRIM41-Mediated Ubiquitination and Degradation of ZSCAN21

(A) 293T cells were co-transfected with FLAG-ZSCAN21 and His-ubiquitin, together with HA-TRIM41, TRIM17-GFP, or both for 24 hr. Then, cells were incubated for 6 hr with 20 μM MG-132. Purified ubiquitinated proteins and input lysates were analyzed by western blot using anti-FLAG, anti-HA, and anti-GFP antibodies.

(B) SH-SY5Y cells were transfected with FLAG-ZSCAN21 in the presence or absence of TRIM17-GFP, FLAG-TRIM41, or both for 24 hr. Then, cells were metabolically labeled with [^{35}S]-Met for 1 hr (pulse) and harvested at the indicated times after washing and incubation in cold culture medium (chase). FLAG-ZSCAN21 was then immunoprecipitated using anti-FLAG beads, separated by SDS-PAGE, and visualized by autoradiography [^{35}S]. The intensity of the bands on the autoradiograms of four independent experiments was quantified. **$p < 0.005$, ***$p = 0.0002$, significantly different from ZSCAN21 alone at given time points ($n = 4$).

(C) SH-SY5Y cells were transfected twice with siRNAs directed against TRIM17 or TRIM41, or with a negative control siRNA for 48 hr. Then, cells were treated with 20 μg/mL cycloheximide for 9 and 15 hr, collected, and analyzed by western blot using anti-ZSCAN21 and anti-actin antibodies. Four western blots from a representative experiment of three independent experiments are shown.

(D) SH-SY5Y cells were transfected as in (C). Then, cells were treated with 20 μg/mL cycloheximide for 24 hr, collected, and analyzed by western blot as in (C). Values in blue represent quantifications of ZSCAN21 protein levels normalized by actin for this experiment. Western blots from a representative experiment of three independent experiments are shown.

(E) The intensity of ZSCAN21 bands on the western blots from three independent experiments performed as in (D) was quantified and normalized with actin. Data are the means ± SDs; *$p = 0.0037$, **$p = 0.0421$, significantly different from the siRNA control.

(F) *In vitro* translated HA-TRIM41 was subjected to *in vitro* ubiquitination assay in the presence of GST or GST-TRIM17. Reactions were analyzed by western blot using anti-HA and anti-GST antibodies.

(G) 293T cells were co-transfected with ZSCAN21-GFP or GFP as a control, together with FLAG-TRIM41, FLAG-TRIM17, or both for 24 hr. GFP-fusion proteins were immunoprecipitated using anti-GFP-trap beads. Immunoprecipitates (IPs) and cell lysates were analyzed by western blot using anti-FLAG and anti-GFP antibodies. The intensity of the HA-TRIM41 band detected in IP was normalized by the intensity of HA-TRIM41 bands detected in total lysates, and the relative values are indicated in blue. Western blots from a representative experiment of three independent experiments are shown.

See also Figure S3.

$n = 3$) in the presence versus the absence of TRIM17 (Figure 4G). This suggests that the inhibitory effect of TRIM17 on ZSCAN21 ubiquitination could be also partly due to the reduced interaction between ZSCAN21 and its E3 ubiquitin ligase TRIM41.

TRIM17, TRIM41, and ZSCAN21 Belong to a Pathway Regulating *SNCA* Expression

To test whether the effects of TRIM17 and TRIM41 on ZSCAN21 stability had an impact on *SNCA* expression level, we used small hairpin RNA (shRNA)-expressing lentiviral particles to specifically knock down the three endogenous proteins in SH-SY5Y cells. Silencing of *ZSCAN21* (Figure 5A) or *TRIM17* (Figure 5B) significantly decreased the mRNA level of *SNCA*, whereas silencing of *TRIM41* significantly increased it (Figure 5C), further supporting the idea that endogenous TRIM17 and TRIM41 antagonistically regulate *SNCA* expression by modulating the protein level of the transcription factor ZSCAN21.

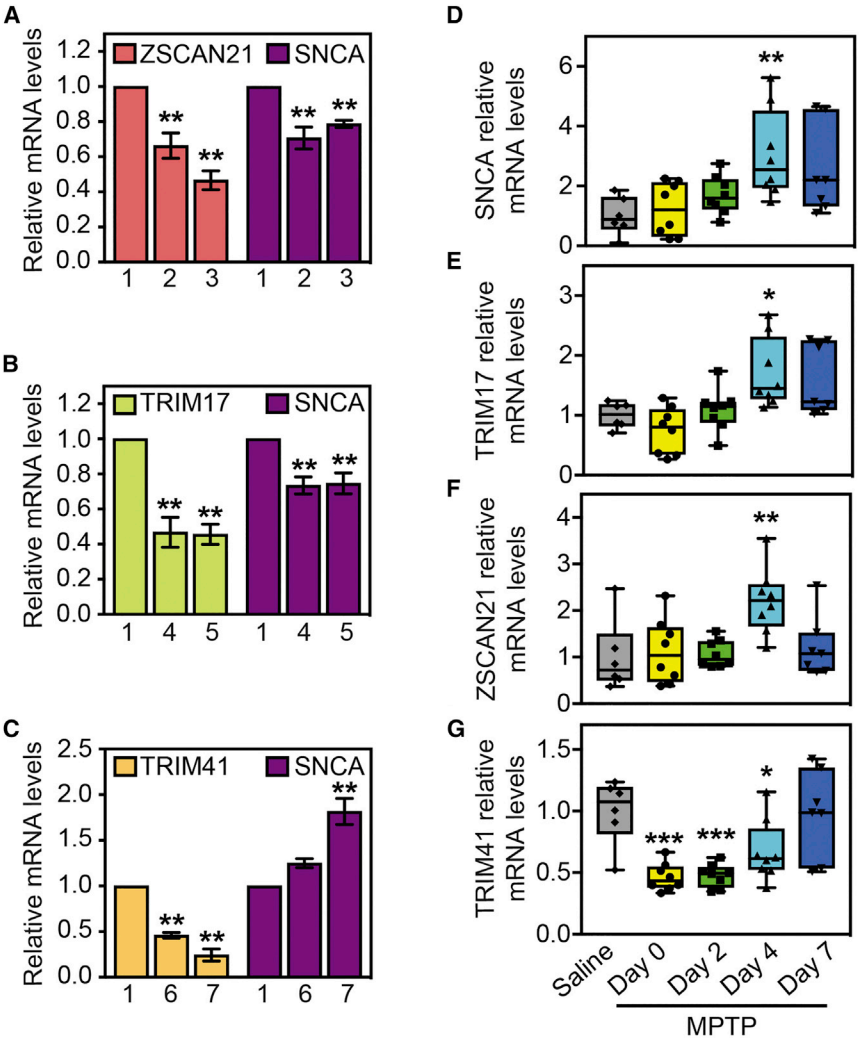

Figure 5. TRIM17, TRIM41, and ZSCAN21 Regulate α-Synuclein Expression

(A–C) SH-SY5Y cells were transduced with lentiviruses expressing a control shRNA (1), or two different specific shRNAs against, respectively, *ZSCAN21* (2 and 3), *TRIM17* (4 and 5), or *TRIM41* (6 and 7). The mRNA levels of endogenous *ZSCAN21* (A), *TRIM17* (B), *TRIM41* (C), and *SNCA* were measured by qPCR. $^{**}p < 0.01$ (n = 4), significantly different from control shRNA.

(D–G) Mice were injected with MPTP or a saline solution following the subacute regimen and were euthanized at different times after the last MPTP injection (0, 2, 4, and 7 days for MPTP- and 7 days for saline-injected mice). The relative mRNA levels of *SNCA* (D) *TRIM17* (E), *ZSCAN21* (F), and *TRIM41* (G) from midbrains were estimated by RT-qPCR. Fold change of each gene was calculated by comparison with the mean of control mice (saline). The graphs show values from individual mice. $^{*}p < 0.05$, $^{**}p < 0.01$, $^{***}p < 0.001$, significantly different from saline.

To assess the *in vivo* relevance of these results, we analyzed the mRNA levels of *TRIM17*, *TRIM41*, *ZSCAN21*, and *SNCA* in a mouse model of PD based on injection of the neurotoxin MPTP. As previously reported (Vila et al., 2000), *SNCA* expression was increased in the midbrains of mice injected with MPTP following a subacute regimen, compared with control mice injected with a saline solution. The *SNCA* mRNA level reached a peak 4 days after the last injection of MPTP (Figure 5D). Consistent with stress-induced expression of *TRIM17* (Lassot et al., 2010) and TRIM17-induced *SNCA* transcription, the mRNA level of *TRIM17* increased simultaneously with *SNCA* (Figure 5E). More unexpected was that *ZSCAN21* mRNA levels also increased following MPTP treatment (Figure 5F) and that *TRIM41* expression was significantly decreased compared to the saline control, early after MPTP treatment (Figure 5G). The protein level of ZSCAN21 may thus increase due to both transcriptional induction and post-translational stabilization (resulting from both TRIM41 downregulation and TRIM17-mediated TRIM41 inhibition), further favoring α-synuclein expression.

These data strongly suggest that ZSCAN21, TRIM17, and TRIM41 belong to a pathway regulating α-synuclein expression in pathological conditions, in which ZSCAN21 is antagonistically regulated by TRIM17 and TRIM41.

Two Variants in *TRIM41* and *ZSCAN21* Genes Co-segregate with Parkinsonism

As TRIM17, TRIM41, and ZSCAN21 regulate the transcription of the *SNCA* gene, mutations in their genes may represent a risk factor for PD. We therefore sequenced the exons and the exon-intron boundaries of the *ZSCAN21*, *TRIM17*, and *TRIM41* genes in 190 index cases from families that were compatible with autosomal dominant PD inheritance, in which *SNCA* multiplications and the leucine-rich repeat kinase 2 (*LRRK2*) G2019S mutation were not found, and 190 healthy French controls. We found a total of nine rare exonic variants: two in *ZSCAN21*, five in *TRIM17*, and two in *TRIM41* (Table S2). Six of these variants were non-synonymous (two in each gene). Except for one *TRIM17* variant, all were predicted to be damaging using *in silico* prediction (Table S2). Segregation analyzes were available for two index cases carrying, respectively, the *ZSCAN21* c.13 G > A, p.V5I variant and the *TRIM41* c.1600 C > T, p.R534C variant, which were found to co-segregate with the disease (Figures 6A and 6C; Table S3). Both were absent from our series of French controls. Furthermore, the *ZSCAN21* c.13 G > A, p.V5I variant was found in an additional familial PD case (Figure 6B). The p.V5I substitution is located in the N-terminal end of ZSCAN21 (Figure 6D), whereas the p.R534C substitution is located in the PRY-SPRY domain of TRIM41 (Figure 6E). Both affected amino acids are at an evolutionary conserved position (Figures 6D and 6E). The p.R534C variation is in a

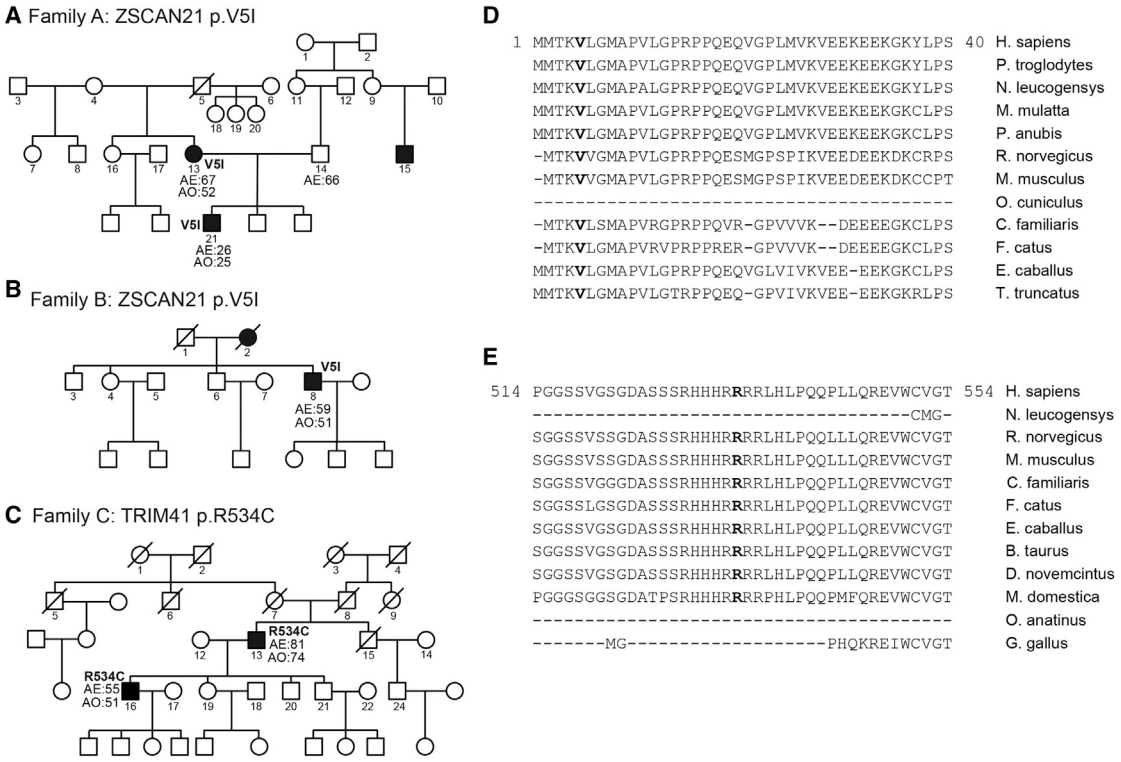

Figure 6. Pedigrees of the Families Carrying the Genetic Variations that Co-segregate with Parkinsonism

(A) Pedigree of the family A carrying the *ZSCAN21* p.V5I variation. AE, age at examination (years); AO, age at onset (years).

(B) Pedigree of the family B carrying the *ZSCAN21* p.V5I variation.

(C) Pedigree of the family C carrying the *TRIM41* p.R534C variation.

(D) Amino acid location of the ZSCAN21 p.V5I variation and sequence alignment with various species.

(E) Amino acid location of TRIM41 p.R534C variation and sequence alignment with various species.

See also Tables S2 and S3.

sequence specific to TRIM41 that is absent in other PRY-SPRY domain-containing TRIM proteins, suggesting a specific role for TRIM41. Clinical characteristics of PD patients with *ZSCAN21 p.V5I* and *TRIM41 p.R534C* variations are reported in the Supplemental Information.

Functional Study of the ZSCAN21 p.V5I and TRIM41 p.R534C Variations

To examine the impact of these variations on the pathway described above, we focused on the two most deleterious, ZSCAN21 p.V5I and TRIM41 p.R534C, based on pathogenicity predictions and co-segregation analyzes. We did not detect any significant difference between the DNA binding of the WT and the p.V5I forms of ZSCAN21 as assessed by a quantitative oligonucleotide pull-down assay from cells transfected with ZSCAN21 constructs fused to Renilla luciferase (Figure 7A). However, ZSCAN21 p.V5I appeared to be slightly but significantly more stable than WT ZSCAN21 in pulse-chase experiments (Figure 7B). The ubiquitination level of ZSCAN21 p.V5I, in the presence of TRIM41, was consistently slightly decreased compared to WT ZSCAN21 (by ~60%; Figures 7C and S4A). The p.V5I variation did not significantly alter the interaction of ZSCAN21 with TRIM17 (Figure S4B), whereas it slightly decreased its interaction with TRIM41 (by ~40%, Figure 7D), as estimated by co-immunoprecipitation. These results suggest that ZSCAN21 p.V5I may be less degraded than WT ZSCAN21 due to a lower affinity for its E3 ubiquitin ligase TRIM41. ZSCAN21 p.V5I may thus induce a higher expression of α-synuclein, while retaining the same affinity for its consensus DNA binding element in the *SNCA* locus.

As *SNCA* is expressed in several hematopoietic lineages in adults such as lymphocytes (Kim et al., 2004; Mutez et al., 2011), we examined its mRNA levels in lymphoblastoid cell lines (LCLs) derived from blood samples of three members of the first family carrying *ZSCAN21 p.V5I* (family A), one from the second family (B8), and one unrelated healthy subject from the control cohort (D1) (Figure 6). *SNCA* expression was slightly but not significantly increased in patients A13 and B8 (with an age at onset older than 50 years) compared to the healthy controls A14 and D1 (Figure 7E). Because α-synuclein expression levels in LCLs may not reflect its expression in dopaminergic neurons and due to the high interindividual variability of α-synuclein expression, we cannot reach conclusions about any pathogenic role of *ZSCAN21 p.V5I* variation from such a limited number of patients. However, it is interesting to note that the level of *SNCA* was strikingly increased (25-fold) in patient A21 (with an age at onset of 25 years)

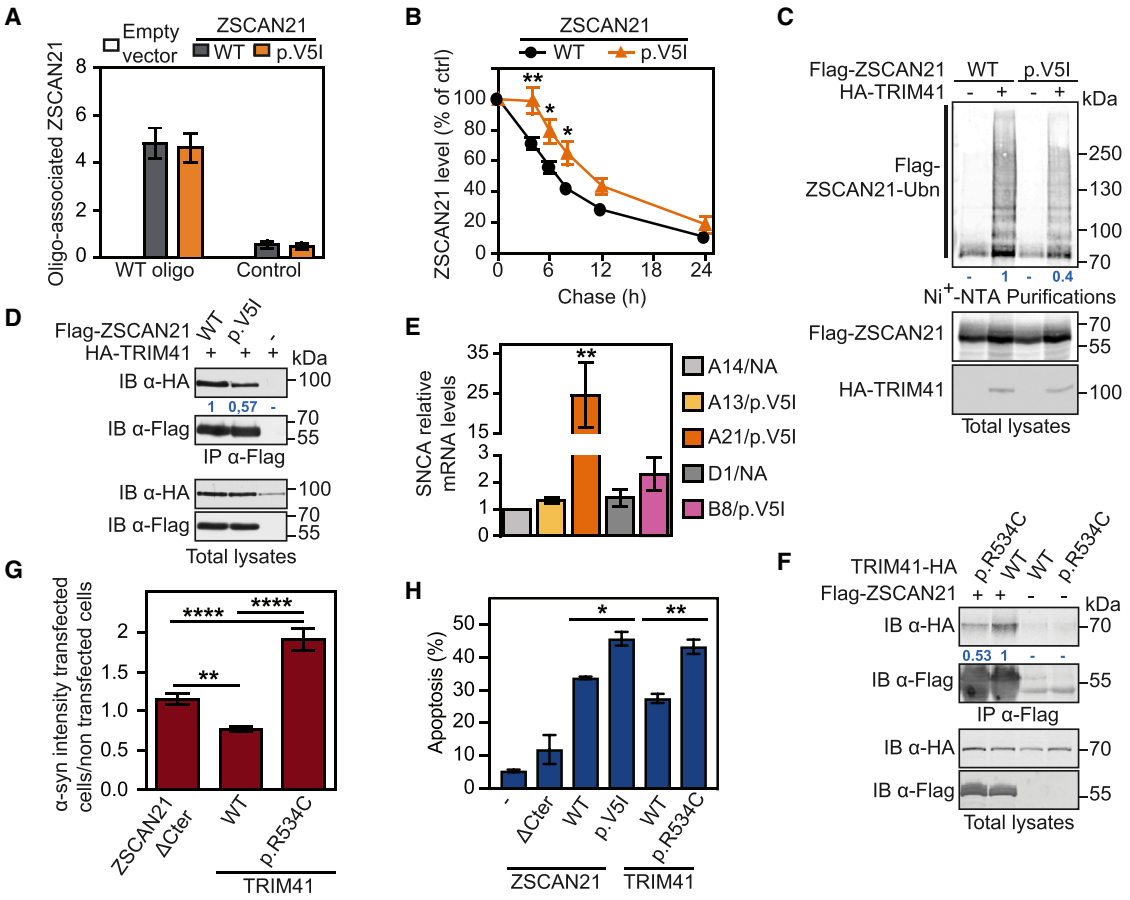

Figure 7. Impact of the ZSCAN21 p.V5I and TRIM41 p.R534C Variants on the ZSCAN21/TRIM17/TRIM41/*SNCA* Pathway

(A) SH-SY5Y cells were transfected with ZSCAN21 (WT or p.V5I)-Renilla luciferase fusion-protein constructs for 24 hr. Then, lysates were incubated with a biotinylated oligonucleotide containing WT or mutant (control) consensus binding site for ZSCAN21, as in Figure 3B. Lysates and precipitates were analyzed by chemoluminescence (n = 5).

(B) SH-SY5Y cells were transfected with FLAG-ZSCAN21 or FLAG-ZSCAN21 p.V5I for 24 hr. Then, cells were metabolically labeled with [^{35}S]-Met for 1 hr (pulse) and harvested at indicated times after washing and incubation in cold culture medium (chase). FLAG-ZSCAN21 was then immunoprecipitated, separated by SDS-PAGE, and visualized by autoradiography [^{35}S]. The intensity of the bands on the autoradiograms of five independent experiments was quantified. *$p < 0.05$, **$p = 0.0016$, significantly different from WT ZSCAN21 at given time points (two-way ANOVA, followed by Sidak's multiple comparison test).

(C) 293T cells were transfected with WT FLAG-ZSCAN21 or FLAG-ZSCAN21 p.V5I together with His-ubiquitinK0 in the presence or absence of HA-TRIM41. Then, cells were incubated for 6 hr with 20 μM MG-132. The ubiquitinated proteins were purified and analyzed by western blot using anti-FLAG antibody. In a separate SDS-PAGE, the input lysates used for the purification were analyzed by western blot using anti-HA and anti-FLAG antibodies. The intensities of the ubiquitinated ladders were normalized by the ZSCAN21 band intensities in total lysates, and their relative values are indicated in blue. Data are representative of four independent experiments. See also Figure S4A.

(D) 293T cells were co-transfected with either WT FLAG-ZSCAN21 or FLAG-ZSCAN21 p.V5I together with HA-TRIM41 and then subjected to immunoprecipitation using an anti-FLAG antibody. Immunoprecipitates (IPs) and cell lysates were analyzed by western blot. Band intensities of co-immunoprecipitated TRIM41 were normalized by band intensities of immunoprecipitated ZSCAN21, and their relative values are indicated in blue. Data are representative of five independent experiments.

(E) The mRNA levels of endogenous *SNCA* in lymphoblastoid cell lines (LCLs) derived from three family A members (A13, A14, and A21), one family B member (B8), and another healthy control (D1) were measured by qPCR. A13, A21, and B8 patients harbor the ZSCAN21 p.V5I variation, whereas healthy controls A14 and D1 do not. **$p < 0.01$, significantly different from A14 (one-way ANOVA, followed by Sidak's multiple comparison test; N = 4).

(F) 293T cells were co-transfected with WT FLAG-ZSCAN21 or with an empty plasmid together with WT HA-TRIM41 or HA-TRIM41 p.R534C. Cell lysates were subjected to immunoprecipitation using anti-FLAG antibody. Immunoprecipitates (IPs) and cell lysates were analyzed by western blot. Band intensities of co-immunoprecipitated TRIM41 were normalized and are indicated as in (D). Data are representative of four independent experiments.

(G) SH-SY5Y cells were transfected with FLAG-ZSCAN21ΔCter, WT HA-TRIM41, or HA-TRIM41 p.534C for 24 hr. Cells were analyzed by immunofluorescence using antibodies against ZSCAN21 or TRIM41, and anti-α-synuclein antibody. Intensity of α-synuclein immunofluorescence was analyzed with Cell Profiler software in each cell. Graph represents the ratio between α-synuclein intensity in ~100 transfected cells, compared to the average of α-synuclein intensity of ~100 non-transfected cells. Only living cells were taken into account. **$p = 0.0031$, ****$p < 0.0001$ (one-way ANOVA, followed by Sidak's multiple comparisons test). Data for ZSCAN21 ΔCter and HA-TRIM41 are the same as in Figure 3E.

(legend continued on next page)

compared to his father (A14), who was not affected by the disease (Figure 7E). In that case, the expression level of *SNCA* correlated with the early age of onset, as already described (Chartier-Harlin et al., 2004; Ibáñez et al., 2004; Singleton et al., 2003).

In parallel, to test the impact of the *TRIM41 p.R534C* substitution, we estimated the intrinsic E3 ubiquitin ligase activity of TRIM41 p.R534C by performing *in vitro* auto-ubiquitination assays. We found no significant difference compared to WT TRIM41 (Figure S4C). In contrast, the TRIM41 p.R534C mutant bound less efficiently to ZSCAN21 than WT TRIM41 (by ~50%), as detected in co-immunoprecipitation experiments (Figure 7F). Therefore, the TRIM41 p.R534C variation may cause reduced ZSCAN21 ubiquitination and degradation and result in increased α-synuclein expression, although it does not alter the E3 ubiquitin ligase activity of TRIM41. Immunofluorescence measurements in individual cells consistently revealed that overexpression of TRIM41 p.R534C significantly increased endogenous α-synuclein expression in SH-SY5Y cells (Figure 7G), compared to untransfected cells, possibly due to a dominant-negative effect leading to ZSCAN21 stabilization. Both ZSCAN21 p.V5I and TRIM41 p.R534C variants induced a higher toxicity when transfected in SH-SY5Y cells, compared to WT ZSCAN21 and WT TRIM41, respectively (Figure 7H), further suggesting a pathogenic effect of both variants.

DISCUSSION

Although accumulating data strongly suggest that increased expression of α-synuclein plays a crucial role in the pathogenesis of PD, the mechanisms regulating the transcription of its gene are mostly unknown. In the present study, we describe a pathway regulating α-synuclein expression in which the stability of the transcription factor ZSCAN21 is antagonistically regulated by two E3 ubiquitin ligases of the TRIM family. We show that ZSCAN21, which binds to a consensus element located in intron 1 of the *SNCA* gene, increases the *SNCA* mRNA level. Our ChIP data are consistent with those of Dermentzaki et al. (2016), showing that ZSCAN21 effectively binds the DNA region within intron 1 of the *SNCA* gene that includes a putative binding site for ZSCAN21 (Clough et al., 2009). Our results in SH-SY5Y cells showing that ZSCAN21 overexpression activates *SNCA* transcription, whereas silencing of *ZSCAN21* decreases it, are also consistent with previous results published by the Stefanis group (Clough et al., 2009; Dermentzaki et al., 2016). However, ZSCAN21 has also been shown to negatively regulate the *SNCA* gene, depending on the cell type and/or the developmental stage studied (Dermentzaki et al., 2016; Wright et al., 2013). Notably, Dermentzaki et al. (2016) reported that silencing of ZSCAN21 increased *SNCA* expression in primary cultures of cortical neurons, whereas it reduced it in neurosphere cultures. In the present study, we show that TRIM41 is an E3 ubiquitin ligase for ZSCAN21 that is inhibited by TRIM17. As TRIM17 is induced in stress conditions (Lassot et al., 2010; Lionnard et al., 2018), it may increase α-synuclein expression in pathological conditions by inhibiting the degradation of ZSCAN21 mediated by TRIM41. We found that TRIM17 overexpression consistently increased α-synuclein expression in SH-SY5Y cells, whereas TRIM41 decreased it. Moreover, knockdown of TRIM17 significantly decreased α-synuclein expression, whereas knockdown of TRIM41 increased it. In line with these results, in the MPTP mouse model of PD, a decrease in *TRIM41* expression levels preceded *SNCA* upregulation; however, *TRIM17* and *ZSCAN21* were induced simultaneously with *SNCA* in the midbrain of mice, further suggesting that TRIM17, TRIM41, and ZSCAN21 are part of a pathway for the transcriptional regulation of α-synuclein.

Our results indicate that TRIM41 acts as an E3 ubiquitin ligase for ZSCAN21. Overexpression of TRIM41 strongly increased the ubiquitination level and decreased the half-life of ZSCAN21, while an inactive mutant of TRIM41 had no effect on ZSCAN21 ubiquitination. The effects of TRIM41 on ZSCAN21 were totally abrogated by TRIM17. This inhibitory effect could be explained by two possible mechanisms. The first mechanism is a direct inhibition of the E3 ubiquitin ligase activity of TRIM41 by TRIM17. This is supported by our data in the present study, showing the inhibition of TRIM41 auto-ubiquitination by TRIM17. This effect may be due to the formation of inactive hetero-oligomers. Several studies have shown that the E3 ubiquitin ligase activity of TRIM proteins requires self-association, notably through dimerization or higher-order oligomerization (Streich et al., 2013) of their RING domains (Koliopoulos et al., 2016). Our data indicate that TRIM17 binds more strongly to TRIM41 than to ZSCAN21. It is therefore plausible that TRIM17 prevents the formation of TRIM41 homo-oligomers and thus inhibits the activity of TRIM41 by forming inactive TRIM17-TRIM41 hetero-oligomers. The second mechanism is the disruption of the TRIM41-ZSCAN21 interaction by TRIM17. TRIM17 reduced the TRIM41-ZSCAN21 interaction when the three proteins were co-expressed and co-immunoprecipitated. These two mechanisms are not mutually exclusive, as formation of TRIM17-TRIM41 hetero-dimers may prevent ZSCAN21 binding to TRIM41. TRIM24 has recently been reported to inhibit the degradation of dysbindin induced by TRIM32 in cardiomyocytes (Borlepawar et al., 2017), indicating that two TRIM proteins can antagonistically regulate the same protein. More importantly, we have recently shown that TRIM17 inhibits TRIM28-mediated degradation of BCL2A1 in a similar way (Lionnard et al., 2018).

As α-synuclein expression is crucial for PD pathogenesis, alterations of genes involved in its transcriptional regulation may represent risk factors. Supporting this hypothesis, we identified rare variants of *TRIM17*, *TRIM41*, and *ZSCAN21* genes in patients with autosomal dominant PD that were absent in healthy controls. Our data show that the ZSCAN21 p.V5I variant is less ubiquitinated by TRIM41 and is more stable than the WT form, suggesting that it could lead to sustained *SNCA* transcription.

(H) SH-SY5Y cells were transfected with WT FLAG-ZSCAN21, FLAG-ZSCAN21 ΔCter, FLAG-ZSCAN21 p.V5I, WT HA-TRIM41, or HA-TRIM41 p.534C for 24 hr. Transfected cells were detected by immunofluorescence using anti-ZSCAN21 or anti-TRIM41 antibodies, and nuclei were stained with DAPI. Apoptosis was estimated in the population of transfected cells by counting cells with condensed nuclei. *p = 0.034, **p = 0.0025 (one-way ANOVA, followed by Sidak's multiple comparisons test).
See also Figure S4.

Likewise, the TRIM41 p.R534C variant interacted with a lower affinity with ZSCAN21 than WT TRIM41, indicating that this variant could be less efficient in mediating the ubiquitination and degradation of ZSCAN21. Overexpression of TRIM41 p.R534C in SH-SY5Y cells consistently significantly increased the endogenous α-synuclein protein level. These data thus support the idea that ZSCAN21 p.V5I and TRIM41 p.R534C variations may lead to increased α-synuclein expression. However, whether these genetic variations have been responsible for PD in patients is presently unknown and further studies are needed to establish any causal link with the disease.

Our results describe a pathway that regulates *SNCA* transcription with *in vivo* and pathological relevance. Notably, our genetic data from patients suggest that a deregulation of this pathway may be involved in the pathogenesis of PD. As such, our study may pave the way for the development of neuroprotective therapeutic strategies aimed at restoring a level of α-synuclein that is compatible with the function and survival of dopaminergic neurons.

STAR★METHODS

Detailed methods are provided in the online version of this paper and include the following:

- KEY RESOURCES TABLE
- CONTACT FOR REAGENT AND RESOURCE SHARING
- EXPERIMENTAL MODEL AND SUBJECT DETAILS
  - Cell cultures and transient transfection
  - Animals
  - Patients and controls
- METHOD DETAILS
  - DNA and sequences
  - Plasmids
  - Materials
  - Yeast two-hybrid screen
  - Western blots
  - GST-TRIM17 pull down assay
  - Transfection and culture of cells
  - Lentiviral transduction of cells
  - Co-immunoprecipitation
  - *In situ* PLA
  - Immunofluorescence
  - Ubiquitination assay
  - Pulse-chase experiments
  - Cycloheximide treatment
  - Chromatin immunoprecipitation (ChIP)
  - Oligonucleotide pull-down assay
  - RNA preparation and RT-qPCR
  - Subacute MPTP intoxication and RNA extraction
  - *In vitro* ubiquitination
  - Sanger sequencing
- QUANTIFICATION AND STATISTICAL ANALYSIS

SUPPLEMENTAL INFORMATION

Supplemental Information includes four figures and four tables and can be found with this article online at https://doi.org/10.1016/j.celrep.2018.11.002.

ACKNOWLEDGMENTS

The authors are grateful to the patients and their families. We thank the DNA and Cell banks of the Institut du Cerveau et de la Moelle épinière (ICM) for DNA preparation. We thank the staff of the Montpellier Genomic Collection platform for providing ZSCAN21 cDNA clones and the Montpellier RIO imaging platform and their financing bodies. We acknowledge the imaging facility Montpellier Resources Imageries (MRI), a member of the national infrastructure France-BioImaging, supported by the French National Research Agency (ANR-10-INBS-04, "Investments for the Future"); S. DeRossi; and B. Monterroso. The His-ubiquitinK0 plasmid was kindly provided by Dr. V. Baldin. We thank Dr. T. Cuadros (Vall d'Hebron Institute of Research [VHIR]) and Dr. E. Martí and T. Zomeño-Abellan (Centre de Regulació Genòmica, Barcelona, Spain) for additional technical assistance on the preparation of samples derived from MPTP-treated animals. We are grateful to Dr. I. Robbins for critical reading of the manuscript. We are also grateful to Hybrigenics for performing the two-hybrid screen. This work was supported by grants from the Association France Parkinson, France; the Fondation de France (PD committee, 2011-00025113; 2012-00034544), France; the Fondation EDF; the Michael J. Fox Foundation for Parkinson's Research (grant ID:12372), US; the Centre National de la Recherche Scientifique (CNRS), France; the Institut National de la Recherche Médicale (INSERM), France and the Université de Montpellier (UM), France.

AUTHOR CONTRIBUTIONS

Conceptualization, I.L. and S.D.; Methodology, I.L. and S.D.; Formal Analysis, S.D. and S.L.; Investigation, I.L., S.M., S.L., B.A.Z., E.C., C.C., J.P.B., B.M., C.M., C.S., C.T., M.V., I.C.-C., A.L., and S.D.; Resources, S.L. and G.M.; Writing, I.L., S.D., and S.L.; Funding Acquisition, I.L., S.D., M.V., and A.B.

DECLARATION OF INTERESTS

The authors declare no competing interests.

Received: April 25, 2017
Revised: October 1, 2018
Accepted: October 30, 2018
Published: November 27, 2018

REFERENCES

Abecasis, G.R., Auton, A., Brooks, L.D., DePristo, M.A., Durbin, R.M., Handsaker, R.E., Kang, H.M., Marth, G.T., and McVean, G.A.; 1000 Genomes Project Consortium (2012). An integrated map of genetic variation from 1,092 human genomes. Nature *491*, 56–65.

Adzhubei, I.A., Schmidt, S., Peshkin, L., Ramensky, V.E., Gerasimova, A., Bork, P., Kondrashov, A.S., and Sunyaev, S.R. (2010). A method and server for predicting damaging missense mutations. Nat. Methods *7*, 248–249.

Borlepawar, A., Rangrez, A.Y., Bernt, A., Christen, L., Sossalla, S., Frank, D., and Frey, N. (2017). TRIM24 protein promotes and TRIM32 protein inhibits cardiomyocyte hypertrophy via regulation of dysbindin protein levels. J. Biol. Chem. *292*, 10180–10196.

Brenner, S., Wersinger, C., and Gasser, T. (2015). Transcriptional regulation of the α-synuclein gene in human brain tissue. Neurosci. Lett. *599*, 140–145.

Carpenter, A.E., Jones, T.R., Lamprecht, M.R., Clarke, C., Kang, I.H., Friman, O., Guertin, D.A., Chang, J.H., Lindquist, R.A., Moffat, J., et al. (2006). CellProfiler: image analysis software for identifying and quantifying cell phenotypes. Genome Biol. *7*, R100.

Chartier-Harlin, M.C., Kachergus, J., Roumier, C., Mouroux, V., Douay, X., Lincoln, S., Levecque, C., Larvor, L., Andrieux, J., Hulihan, M., et al. (2004). Alpha-synuclein locus duplication as a cause of familial Parkinson's disease. Lancet *364*, 1167–1169.

Chen, D., Gould, C., Garza, R., Gao, T., Hampton, R.Y., and Newton, A.C. (2007). Amplitude control of protein kinase C by RINCK, a novel E3 ubiquitin ligase. J. Biol. Chem. *282*, 33776–33787.

Clough, R.L., and Stefanis, L. (2007). A novel pathway for transcriptional regulation of alpha-synuclein. FASEB J. *21*, 596–607.

Clough, R.L., Dermentzaki, G., and Stefanis, L. (2009). Functional dissection of the alpha-synuclein promoter: transcriptional regulation by ZSCAN21 and ZNF219. J. Neurochem. *110*, 1479–1490.

Corti, O., Lesage, S., and Brice, A. (2011). What genetics tells us about the causes and mechanisms of Parkinson's disease. Physiol. Rev. *91*, 1161–1218.

Cronin, K.D., Ge, D., Manninger, P., Linnertz, C., Rossoshek, A., Orrison, B.M., Bernard, D.J., El-Agnaf, O.M., Schlossmacher, M.G., Nussbaum, R.L., and Chiba-Falek, O. (2009). Expansion of the Parkinson disease-associated SNCA-Rep1 allele upregulates human alpha-synuclein in transgenic mouse brain. Hum. Mol. Genet. *18*, 3274–3285.

Dehay, B., Bourdenx, M., Gorry, P., Przedborski, S., Vila, M., Hunot, S., Singleton, A., Olanow, C.W., Merchant, K.M., Bezard, E., et al. (2015). Targeting α-synuclein for treatment of Parkinson's disease: mechanistic and therapeutic considerations. Lancet Neurol. *14*, 855–866.

Dermentzaki, G., Paschalidis, N., Politis, P.K., and Stefanis, L. (2016). Complex effects of the ZSCAN21 transcription factor on transcriptional regulation of alpha-synuclein in primary neuronal cultures and in vivo. J. Biol. Chem. *291*, 8756–8772.

Devine, M.J., Ryten, M., Vodicka, P., Thomson, A.J., Burdon, T., Houlden, H., Cavaleri, F., Nagano, M., Drummond, N.J., Taanman, J.W., et al. (2011). Parkinson's disease induced pluripotent stem cells with triplication of the α-synuclein locus. Nat. Commun. *2*, 440.

Duplan, E., Giordano, C., Checler, F., and Alves da Costa, C. (2016). Direct α-synuclein promoter transactivation by the tumor suppressor p53. Mol. Neurodegener. *11*, 13.

Farrer, M., Kachergus, J., Forno, L., Lincoln, S., Wang, D.S., Hulihan, M., Maraganore, D., Gwinn-Hardy, K., Wszolek, Z., Dickson, D., and Langston, J.W. (2004). Comparison of kindreds with parkinsonism and alpha-synuclein genomic multiplications. Ann. Neurol. *55*, 174–179.

Formstecher, E., Aresta, S., Collura, V., Hamburger, A., Meil, A., Trehin, A., Reverdy, C., Betin, V., Maire, S., Brun, C., et al. (2005). Protein interaction mapping: a Drosophila case study. Genome Res. *15*, 376–384.

Fromont-Racine, M., Rain, J.C., and Legrain, P. (1997). Toward a functional analysis of the yeast genome through exhaustive two-hybrid screens. Nat. Genet. *16*, 277–282.

Gründemann, J., Schlaudraff, F., Haeckel, O., and Liss, B. (2008). Elevated alpha-synuclein mRNA levels in individual UV-laser-microdissected dopaminergic substantia nigra neurons in idiopathic Parkinson's disease. Nucleic Acids Res. *36*, e38.

Hughes, A.J., Daniel, S.E., Kilford, L., and Lees, A.J. (1992). Accuracy of clinical diagnosis of idiopathic Parkinson's disease: a clinico-pathological study of 100 cases. J. Neurol. Neurosurg. Psychiatry *55*, 181–184.

Ibáñez, P., Bonnet, A.M., Débarges, B., Lohmann, E., Tison, F., Pollak, P., Agid, Y., Dürr, A., and Brice, A. (2004). Causal relation between alpha-synuclein gene duplication and familial Parkinson's disease. Lancet *364*, 1169–1171.

Jowaed, A., Schmitt, I., Kaut, O., and Wüllner, U. (2010). Methylation regulates alpha-synuclein expression and is decreased in Parkinson's disease patients' brains. J. Neurosci. *30*, 6355–6359.

Kim, S., Jeon, B.S., Heo, C., Im, P.S., Ahn, T.B., Seo, J.H., Kim, H.S., Park, C.H., Choi, S.H., Cho, S.H., et al. (2004). Alpha-synuclein induces apoptosis by altered expression in human peripheral lymphocyte in Parkinson's disease. FASEB J. *18*, 1615–1617.

Kimura, T., Mandell, M., and Deretic, V. (2016). Precision autophagy directed by receptor regulators - emerging examples within the TRIM family. J. Cell Sci. *129*, 881–891.

Kircher, M., Witten, D.M., Jain, P., O'Roak, B.J., Cooper, G.M., and Shendure, J. (2014). A general framework for estimating the relative pathogenicity of human genetic variants. Nat. Genet. *46*, 310–315.

Koliopoulos, M.G., Esposito, D., Christodoulou, E., Taylor, I.A., and Rittinger, K. (2016). Functional role of TRIM E3 ligase oligomerization and regulation of catalytic activity. EMBO J. *35*, 1204–1218.

Lassot, I., Robbins, I., Kristiansen, M., Rahmeh, R., Jaudon, F., Magiera, M.M., Mora, S., Vanhille, L., Lipkin, A., Pettmann, B., et al. (2010). Trim17, a novel E3 ubiquitin-ligase, initiates neuronal apoptosis. Cell Death Differ. *17*, 1928–1941.

Linnertz, C., Saucier, L., Ge, D., Cronin, K.D., Burke, J.R., Browndyke, J.N., Hulette, C.M., Welsh-Bohmer, K.A., and Chiba-Falek, O. (2009). Genetic regulation of alpha-synuclein mRNA expression in various human brain tissues. PLoS One *4*, e7480.

Lionnard, L., Duc, P., Brennan, M.S., Kueh, A.J., Pal, M., Guardia, F., Mojsa, B., Damiano, M.A., Mora, S., Lassot, I., et al. (2018). TRIM17 and TRIM28 antagonistically regulate the ubiquitination and anti-apoptotic activity of BCL2A1. Cell Death Differ. Published online July 24, 2018. https://doi.org/10.1038/s41418-018-0169-5.

Magiera, M.M., Mora, S., Mojsa, B., Robbins, I., Lassot, I., and Desagher, S. (2013). Trim17-mediated ubiquitination and degradation of Mcl-1 initiate apoptosis in neurons. Cell Death Differ. *20*, 281–292.

Masliah, E., Rockenstein, E., Veinbergs, I., Mallory, M., Hashimoto, M., Takeda, A., Sagara, Y., Sisk, A., and Mucke, L. (2000). Dopaminergic loss and inclusion body formation in alpha-synuclein mice: implications for neurodegenerative disorders. Science *287*, 1265–1269.

Meroni, G., and Diez-Roux, G. (2005). TRIM/RBCC, a novel class of 'single protein RING finger' E3 ubiquitin ligases. BioEssays *27*, 1147–1157.

Miller, D.W., Hague, S.M., Clarimon, J., Baptista, M., Gwinn-Hardy, K., Cookson, M.R., and Singleton, A.B. (2004). Alpha-synuclein in blood and brain from familial Parkinson disease with SNCA locus triplication. Neurology *62*, 1835–1838.

Mojsa, B., Mora, S., Bossowski, J.P., Lassot, I., and Desagher, S. (2015). Control of neuronal apoptosis by reciprocal regulation of NFATc3 and Trim17. Cell Death Differ. *22*, 274–286.

Mutez, E., Leprêtre, F., Le Rhun, E., Larvor, L., Duflot, A., Mouroux, V., Kerckaert, J.P., Figeac, M., Dujardin, K., Destée, A., and Chartier-Harlin, M.C. (2011). SNCA locus duplication carriers: from genetics to Parkinson disease phenotypes. Hum. Mutat. *32*, E2079–E2090.

Nuber, S., Harmuth, F., Kohl, Z., Adame, A., Trejo, M., Schönig, K., Zimmermann, F., Bauer, C., Casadei, N., Giel, C., et al. (2013). A progressive dopaminergic phenotype associated with neurotoxic conversion of α-synuclein in BAC-transgenic rats. Brain *136*, 412–432.

Rual, J.F., Venkatesan, K., Hao, T., Hirozane-Kishikawa, T., Dricot, A., Li, N., Berriz, G.F., Gibbons, F.D., Dreze, M., Ayivi-Guedehoussou, N., et al. (2005). Towards a proteome-scale map of the human protein-protein interaction network. Nature *437*, 1173–1178.

Scherzer, C.R., Grass, J.A., Liao, Z., Pepivani, I., Zheng, B., Eklund, A.C., Ney, P.A., Ng, J., McGoldrick, M., Mollenhauer, B., et al. (2008). GATA transcription factors directly regulate the Parkinson's disease-linked gene alpha-synuclein. Proc. Natl. Acad. Sci. USA *105*, 10907–10912.

Schindelin, J., Arganda-Carreras, I., Frise, E., Kaynig, V., Longair, M., Pietzsch, T., Preibisch, S., Rueden, C., Saalfeld, S., Schmid, B., et al. (2012). Fiji: an open-source platform for biological-image analysis. Nat. Methods *9*, 676–682.

Sievers, F., Wilm, A., Dineen, D., Gibson, T.J., Karplus, K., Li, W., Lopez, R., McWilliam, H., Remmert, M., Söding, J., et al. (2011). Fast, scalable generation of high-quality protein multiple sequence alignments using Clustal Omega. Mol. Syst. Biol. *7*, 539.

Singleton, A.B., Farrer, M., Johnson, J., Singleton, A., Hague, S., Kachergus, J., Hulihan, M., Peuralinna, T., Dutra, A., Nussbaum, R., et al. (2003). alpha-Synuclein locus triplication causes Parkinson's disease. Science *302*, 841.

Stefanis, L. (2012). α-Synuclein in Parkinson's disease. Cold Spring Harb. Perspect. Med. *2*, a009399.

Streich, F.C., Jr., Ronchi, V.P., Connick, J.P., and Haas, A.L. (2013). Tripartite motif ligases catalyze polyubiquitin chain formation through a cooperative allosteric mechanism. J. Biol. Chem. *288*, 8209–8221.

Sunkin, S.M., Ng, L., Lau, C., Dolbeare, T., Gilbert, T.L., Thompson, C.L., Hawrylycz, M., and Dang, C. (2013). Allen Brain Atlas: an integrated spatio-temporal portal for exploring the central nervous system. Nucleic Acids Res. *41*, D996–D1008.

Swainson, L., Mongellaz, C., Adjali, O., Vicente, R., and Taylor, N. (2008). Lentiviral transduction of immune cells. Methods Mol. Biol. *415*, 301–320.

Urano, T., Usui, T., Takeda, S., Ikeda, K., Okada, A., Ishida, Y., Iwayanagi, T., Otomo, J., Ouchi, Y., and Inoue, S. (2009). TRIM44 interacts with and stabilizes terf, a TRIM ubiquitin E3 ligase. Biochem. Biophys. Res. Commun. *383*, 263–268.

Vila, M., Vukosavic, S., Jackson-Lewis, V., Neystat, M., Jakowec, M., and Przedborski, S. (2000). Alpha-synuclein up-regulation in substantia nigra dopaminergic neurons following administration of the parkinsonian toxin MPTP. J. Neurochem. *74*, 721–729.

Woodsmith, J., Jenn, R.C., and Sanderson, C.M. (2012). Systematic analysis of dimeric E3-RING interactions reveals increased combinatorial complexity in human ubiquitination networks. Mol.Cell. Proteomics *11*, M111.016162.

Wright, J.A., McHugh, P.C., Pan, S., Cunningham, A., and Brown, D.R. (2013). Counter-regulation of alpha- and beta-synuclein expression at the transcriptional level. Mol. Cell. Neurosci. *57*, 33–41.

Yamada, M., Iwatsubo, T., Mizuno, Y., and Mochizuki, H. (2004). Overexpression of alpha-synuclein in rat substantia nigra results in loss of dopaminergic neurons, phosphorylation of alpha-synuclein and activation of caspase-9: resemblance to pathogenetic changes in Parkinson's disease. J. Neurochem. *91*, 451–461.

Yang, X.W., Zhong, R., and Heintz, N. (1996). Granule cell specification in the developing mouse brain as defined by expression of the zinc finger transcription factor RU49. Development *122*, 555–566.

STAR★METHODS

KEY RESOURCES TABLE

REAGENT or RESOURCE	SOURCE	IDENTIFIER
Antibodies		
GFP-Trap®-A beads	Chromotek	Cat#gta-20; RRID:AB_2631357
Rat monoclonal anti-RFP antibody, clone 5F8	Chromotek	Cat#5f8-100; RRID:AB_2336064
Rabbit anti-GFP antibody	Torrey Pines	Cat#TP401; RRID:AB_10013661
Mouse monoclonal antibody anti-Actin, clone C4	Millipore	Cat#MAB1501; RRID:AB_2223041
Anti-FlagM2® affinity gel	Sigma-Aldrich	Cat#A2220; RRID:AB_10063035
Mouse monoclonal anti-Flag®, clone M2	Sigma-Aldrich	Cat#F3165; RRID:AB_259529
Rabbit affinity isolated anti-TRIM41	Sigma-Aldrich	Cat#HPA024204; RRID:AB_1858299
Rabbit affinity isolated anti-ZSCAN21	Sigma-Aldrich	Cat#HPA023591; RRID:AB_1859037
Rabbit anti-mouse ZIPRO1 (ZSCAN21)	Millipore	Cat#AB3733, RRID:AB_11210165
Mouse anti-human ZSCAN21, clone OTI3D4	Cliniscience	Cat#TA506147; RRID:AB_2623640
Monoclonal anti-alpha-Tubulin, clone DM1A	Sigma-Aldrich	Cat#T6199; RRID:AB_477583
Purified anti-peptide antibody against human TRIM17	Eurogentech, this paper	N/A
Rabbit anti-human TRIM41 antibody	Abcam	Cat#ab98170; RRID:AB_10672571
Purified mouse anti-human MCL-1	BD Biosciences	Cat#559027; RRID:AB_397176
Purified mouse anti-α-synuclein	BD Biosciences	Cat#610787; RRID:AB_398108
Mouse monoclonal anti-HA, clone 12CA5	Sigma-Aldrich	Cat#11583816001; RRID:AB_514505
Rat monoclonal anti-HA high affinity, clone 3F10	Sigma-Aldrich	Cat#11867423001; RRID:AB_10094468
Rabbit monoclonal antibody anti-c-Jun, clone 60A8	Cell Signaling Technology	Cat#9165; RRID:AB_2130165
Rabbit polyclonal anti-ubiquitin	Dako	Cat#Z0458; RRID:AB_2315524
Critical commercial reagents		
MagneHis™ Ni-Particles	Promega	Cat#V8611
MagneGST Particles	Promega	Cat#V8565
Easy Tag Methionine L-[^{35}S]	Perkin Elmer	Cat#NEG709A
Lipofectamine 2000 Transfection Kit	Thermo Fisher Scientific	Cat#11668027
Lipofectamine RNAiMax Kit	Thermo Fisher Scientific	Cat#13778075
GenJet transfection reagent Ver.II	SignaGen Laboratories	Cat#SL100489
Dual-Luciferase assay kit	Promega	Cat#E1960
RNAqueous® kits, Ambion	Thermofisher Scientific	Cat#AM1912 and AM1931
DNA-free DNA Removal Kit	Thermofisher Scientific	Cat#AM1906
miRNeasy Mini Kit	QIAGEN	Cat#T217004
TNT® SP6 coupled wheat germ extract system	Promega	Cat#L5030
1-methyl-4-phenyl-1,2,3,6-tetrahydropyridine (MPTP)-HCl	Sigma-Aldrich	Cat#M0896
Duolink® *In Situ* PLA® Probe Anti-Mouse MINUS Affinity purified Donkey anti-Mouse IgG (H+L)	Sigma-Aldrich	Cat#DUO92004
Duolink® *In Situ* PLA® Probe Anti-Rabbit PLUS Affinity purified Donkey anti-Rabbit IgG (H+L)	Sigma-Aldrich	Cat#DUO920042
Duolink® *In Situ* Detection Reagents Green	Sigma-Aldrich	Cat#DUO92014
Streptavidin-agarose beads	Sigma-Aldrich	Cat#85881
Bacterial and Virus Strains		
pLKO.1-shRNA-control#1	Sigma-Aldrich	Cat#SHC002
pLKO.1-shRNA-ZSCAN21#2	Sigma-Aldrich	Cat#TRCN0000015019
pLKO.1-shRNA-ZSCAN21#3	Sigma-Aldrich	Cat#TRCN0000015022
pLKO.1-shRNA-TRIM17#4	Sigma-Aldrich	Cat#TRCN0000033825
pLKO.1-shRNA-TRIM17#5	Sigma-Aldrich	Cat#TRCN0000033828

(*Continued on next page*)

Continued

REAGENT or RESOURCE	SOURCE	IDENTIFIER
pLKO.1-shRNA-TRIM41#6	Sigma-Aldrich	Cat#TRCN0000034045
pLKO.1-shRNA-TRIM41#7	Sigma-Aldrich	Cat#TRCN0000247961
Chemicals, Peptides, and Recombinant Proteins		
GST-TRIM17 (mouse)	This paper	N/A
GST-TRIM17 (human)	This paper	N/A
MG-132	Sigma-Aldrich	Cat#474790
Cycloheximide	Sigma-Aldrich	Cat#C1988
Human recombinant His-tagged ubiquitin-activating enzyme E1	BostonBiochem	Cat#E-304
Human recombinant His-tagged ubiquitin-conjugating enzyme (E2) (Ube2d3)	BioMol International	Cat# U0880
Ubiquitin Nterminal-Histidine tagged	Sigma-Aldrich	Cat#U5507
Experimental Models: Cell Lines		
SH-SY5Y	ATCC	Cat# CRL-2266, RRID:CVCL_0019
Lenti-X 293T	Clontech	Cat#632/80
Lymphoblastoïd cell lines from patients	This paper	N/A
Experimental Models: Organisms/Strains		
Mouse: WT C57BL/6	Charles River	N/A
Bacteria: *Escherichia coli* BL21	New England Biolabs	Cat#C2527I
Oligonucleotides		
See Table S4 for oligonucleotides information	N/A	N/A
SiRNA targeting sequence: TRIM41#1: AAGGAGACT TTCAATAGGTGT	Integrated DNA Technologies	N/A
SiRNA targeting sequence: TRIM41#2: CAGACCGG CCAGAATTTAG	Integrated DNA Technologies	N/A
SiRNA targeting sequence: TRIM17#1: GAACGCATT GTGCTGGAGTTTC	Integrated DNA Technologies	N/A
SiRNA targeting sequence: TRIM17#2: GGTATACTG ACAGATGCTT	Integrated DNA Technologies	N/A
SiRNA targeting sequence: Control: TCGAAGTATTC CGCGTACG	Integrated DNA Technologies	N/A
PCR Primer on ChIP, forward: 5′-AGCAGAGGGACTC AGGTAAG-3′	Integrated DNA Technologies	N/A
PCR Primer on ChIP, reverse: 5′-GCTCCCCAAAGGG ACAAGTA-3′	Integrated DNA Technologies	N/A
Oligonucleotide used in pull down, WT forward: 5′- TAGGGAGCCGGTAAGTACCTGTAGATG-3′	Integrated DNA Technologies	N/A
Oligonucleotide used in pull down, WT reverse: 5′- CATCTACAGGTACTTACCGGCTCCCTA-3	Integrated DNA Technologies	N/A
Oligonucleotide used in pull down, mutant forward: 5′- TAGGGAGCCGGTAAAAAACTGTAGATG −3′	Integrated DNA Technologies	N/A
Oligonucleotide used in pull down, mutant reverse: 5′- CATCTACAGTTTTTTACCGGCTCCCTA-3′.	Integrated DNA Technologies	N/A
Recombinant DNA		
Plasmid: pLexA-Trim17	Mojsa et al., 2015	N/A
Plasmid: pci-3xFlag-TRIM17 and mutants	This paper	N/A
Plasmid: pGEX4T1-mouse TRIM17	Lassot et al., 2010	N/A
Plasmid: pGEX4T1-mouse TRIM17	This paper	N/A
Plasmid: pci-3xFlag-ZSCAN21 and mutants	This paper	N/A
Plasmid: pci-TRIM17-GFP and p.C16A mutant	Lionnard et al., 2018	N/A

(*Continued on next page*)

Continued

REAGENT or RESOURCE	SOURCE	IDENTIFIER
Plasmid: pci-ZSCAN21-GFP	This paper	N/A
Plasmid: pCS2-HA-Trim41 and mutants	This paper	N/A
Plasmid: pci-3xFlag-Trim41 and mutants	This paper	N/A
Plasmid: pcDNA-renilla-HA-ZSCAN21 and p.V5I mutant	This paper	N/A
Plasmid: pci-TRIM44-cherry	This paper	N/A
Plasmid: pCS2-HA-TRIM44	This paper	N/A
Plasmid: pCS2-HA-TRIM17	This paper	N/A
Plasmid: pci-3xFlag-TRIM39	This paper	N/A
Plasmid: TRIM39 cherry	This paper	N/A
Plasmid: HA-TRIM5a	This paper	N/A
Software and Algorithms		
Cell profiler	Carpenter et al., 2006	Cellprofiler.org
Fiji	Schindelin et al., 2012	https://fiji.sc
Imaris		http://www.bitplane.com
MxPro software (Agilent)		https://www.genomics.agilent.com/GenericB.aspx?PageType=Custom&SubPageType=Custom&PageID=2100
PolyPhen2	Adzhubei et al., 2010	http://genetics.bwh.harvard.edu
CADD prediction software	Kircher et al., 2014	https://cadd.gs.washington.edu
The ClustalW program on the European Bioinformatics Institute server	Sievers et al., 2011	https://www.ebi.ac.uk/clustalw

CONTACT FOR REAGENT AND RESOURCE SHARING

Further information and requests for resources and reagents should be directed to and will be fulfilled by the Lead Contact, Iréna Lassot (irena.lassot@igmm.cnrs.fr).

EXPERIMENTAL MODEL AND SUBJECT DETAILS

Cell cultures and transient transfection

293T, Neuro2A, U2OS and SH-SY5Y cell lines were grown in Dulbecco's modified Eagle's medium containing 4.5 g/l glucose supplemented with 5 to 10% fetal bovine serum and penicillin-streptomycin 100 IU/ml-100 μg/ml.

Animals

WT male C57BL/6 mice (8-10 weeks old; Charles River, Lyon, France) were housed under controlled conditions with *ad libitum* access to food and water during a 12 hours (hr) light/dark cycle. All procedures were conducted in accordance with standard ethical guidelines (EU regulations L35/118/12/1986; Ethical Committee for the Use of Laboratory Animals in Spain 53/2013) and approved by the Vall d'Hebron Research Institute (VHIR) Ethical Experimentation Committee.

Patients and controls

We selected 190 index cases of European origin, mostly from France (90%), from a population of 510 PD families compatible with autosomal dominant inheritance. We excluded the leucine-rich repeat kinase 2 (*LRRK2*) G2019S mutation and *SNCA* multiplications in all 190 index cases. PD was diagnosed according to the UK Parkinson's Disease Society Brain Bank (PDSBB) clinical diagnostic criteria (Hughes et al., 1992). Most PD cases (> 70%) had definite PD. The mean age at disease onset (AO) in the 86 female and 104 male index patients was 50.6 ± 11.9 years (range 14-86) and their age at examination was 58.4 ± 11.8 years (range 24-87). One hundred and ninety control subjects, of European origin (57% males, mainly spouses), with no family histories of PD, were examined at age 58.1 ± 11.8 (range 31-85). Informed consent was obtained from all participants and the genetic studies were approved by local ethics committees (INSERM, Protocole Projet RBM 03-48, CCPPRB du Groupe Hospitalier Pitié-Salpêtrière, Paris, France).

METHOD DETAILS

DNA and sequences

Human TRIM17 (GenBank: NM_016102); mouse Trim17 (GenBank: NM_031172); Human TRIM41 (GenBank: NM_033549.4); mouse Trim41 (GenBank: NM_145377.2); Human ZSCAN21 (GenBank: NM_145914.2); mouse Zscan21 (GenBank: NM_011757.3); ZSCAN21 proteins (GenPept: NP_666019.1, NP_001038168, NP_001129089.1, XP_003278116.1, XP_001099737.1, XP_017811700.1, NP_001012021.1, XP_008247126.1, XP_006942058.1, XP_005598663.1, XP_004318912.1); TRIM41 proteins (GenPept: NP_291027.3, NP_663352, XP_003279628.3, NP_001128209.1, XP_005626338.1, XP_006927550.1, XP_014585924.1, NP_001193094.1, XP_004468623, XP_001372311.1, NP_001025843.1); Genomic sequences of *SNCA* (GenBank: NC_000004.12; NC_027897.1, NC_000072.6, NC_005103.4, NC_013683.1, NC_019463.2).

Plasmids

GST-Trim17 vector expressing GST fused to the N-terminus of mouse Trim17 was previously described (Lassot et al., 2010). The cDNAs of human TRIM17 and human ZSCAN21, C-terminally fused to GFP in the pEGFP plasmid, and HA-TRIM5α expressing vector were obtained from the ORFeome library (Montpellier Genomic Collection-MGC facility) and amplified by PCR. Fragments corresponding to untagged TRIM17 and ZSCAN21 cDNAs were then cloned into pCI-3 × Flag plasmid to fuse 3 × Flag tag in the N-terminal ends of TRIM17 and ZSCAN21. Otherwise, TRIM17-GFP cDNA and ZSCAN21-GFP were cloned in the pCI plasmid after PCR amplification. The TRIM17 p.C16A-GFP mutant was obtained by site-directed mutagenesis of pCI-TRIM17-GFP using corresponding primers. The deletion mutants of human ZSCAN21 were constructed by PCR on pCI-3 × Flag-ZSCAN21 plasmid. Amplicons were subsequently cloned into the pCI-3 × Flag plasmid. The Flag-ZSCAN21 p.V5I and HA-TRIM41 p.R534C mutants were obtained by site-directed mutagenesis of pCI-3 × Flag-ZSCAN21 or pCS2-HA-TRIM41 plasmids respectively. Plasmids expressing *Renilla* luciferase fused to the N-terminal end of either WT ZSCAN21 or the ZSCAN21 p.V5I mutant were obtained by cloning the corresponding cDNAs from Orfeome clones into pcDNA-renilla-HA plasmid using Gateway technology (Invitrogen). Mouse cDNA of TRIM41 (GenBank: NM_145377.2), TRIM39 (GenBank: NM_024468), TRIM44 (GenBank: NM_020267) and ZSCAN21 (GenBank: NM_011757) were amplified from a homemade cDNA library by PCR. Amplicons were then sub-cloned into pCI-3 × Flag and/or pCS2-HA plasmids between EcoRI and XhoI or XbaI sites. HA-TRIM41(ΔRING) was obtained by site-directed mutagenesis from pCS2-HA-TRIM41 plasmid. Plasmids expressing mouse ZSCAN21(ΔCter) and Zinc-fingers domain of mouse ZSCAN21 (Zn-fg) with an N-terminal FLAG tag were obtained by PCR and subsequent cloning into the pCI-3 × Flag plasmid. A TRIM44 fragment with a mCherry overhang, and a mCherry fragment with a TRIM44 overhang were amplified by PCR using pCS2-HA-TRIM44 and pmCherry (Clontech) as templates and primer pairs described below. The two amplicons from PCR 1 and PCR 2 were purified, mixed and used as template for a third PCR amplification. The resulting amplicon was cloned into pCI to create the pCI-TRIM44-mCherry plasmid. See Table S4 for PCR primer pairs used for constructs.

Materials

Culture media were from GIBCO® Life technologies. Fetal calf serum, other culture reagents, protease inhibitor cocktail, DAPI, MG-132 and other chemicals were from Sigma-Aldrich. GFP-Trap®-A beads (catalog # gta-20, 10 μl) and rat monoclonal anti-RFP antibody (clone 5F8, catalog # 5f8-100, 1:1000) were from Chromotek. Rabbit anti-GFP antibody was from Torrey Pines (catalog # TP401; 1:5000). Mouse monoclonal antibody against actin (clone C4, catalog # MAB1501, 1:5000) and rabbit anti-mouse ZSCAN21 (Catalog # AB3733, discontinued) were from Millipore. Gel affinity anti-FlagM2® agarose beads (catalog # A2220, 15 μl), mouse monoclonal anti-Flag® (clone M2, catalog # F3165), rabbit affinity isolated anti-TRIM41 (catalog # HPA024204), rabbit affinity isolated anti-human ZSCAN21 (catalog # HPA023591), mouse monoclonal anti-HA (clone 12CA5, catalog #11583816001), rat monoclonal anti-HA high affinity (clone 3F10, catalog #11867423001) and mouse monoclonal anti-tubulin (clone DM1A, catalog # T6199) antibodies were from Sigma-Aldrich. Mouse monoclonal anti-human ZSCAN21 (clone OTI3D4, catalog # AB3733) was from Cliniscience. Purified anti-peptide antibody against human TRIM17 was a custom antibody generated by Eurogentech; Rabbit anti-human TRIM41 antibody used in Figure 3I was from Abcam (Catalog # ab98170) and anti-human MCL-1 was from BD (Catalog # 559027, BD Biosciences). Rabbit monoclonal antibody against c-Jun (clone 60A8) was from Cell Signaling Technology (Catalog # 9165). Rabbit polyclonal anti-ubiquitin was from Dako (Catalog # Z0458). Horseradish peroxidase-conjugated (1:10000) mouse and goat anti-rabbit (Catalog # 211-032-171 and 111-035-144), goat anti-rat (Catalog # 112-035-175 and 112-035-143) and goat anti-mouse (Catalog # 115-035-174 and 115-035-071) secondary antibodies Light Chain specific or AffiniPure were from Jackson ImmunoResearch Laboratories Inc. Fluorescent conjugated antibodies (1:5000): Goat anti-Rabbit secondary antibody Dylight680 conjugate (Catalog # 35568, 1:5000), goat anti-mouse Dylight680 conjugate (Catalog # 35518), goat anti-Rat Dylight680 conjugate (Catalog # SA510022), goat anti-Rabbit secondary antibody Dylight800 conjugate (Catalog # SA535571), goat anti-Mouse Dylight800 conjugate (Catalog # SA535521) and goat anti-Rat Dylight800 conjugate (Catalog #SA510024) were from ThermoFischer Scientific. For immunofluorescence experiments, Alexa Fluor 488 and Alexa Fluor 594-labeled goat anti-mouse (Catalog # A-11029 and A-11032) and goat anti-rabbit (Catalog # A-11034 and A-11012) antibodies were from Molecular Probes, Invitrogen.

Yeast two-hybrid screen

Yeast two-hybrid screening was performed by Hybrigenics SA, Paris, France (https://www.hybrigenics-services.com) as previously described in Mojsa et al. (Mojsa et al., 2015). The coding sequence for amino acids 2-447 of the mouse Trim17 protein (GenBank: NM_031172) was PCR-amplified and cloned into pB27 as a C-terminal fusion to LexA (N-LexA-Trim17-C). The construct was used as a bait to screen a random-primed mouse, embryonic brain (E10.5-E12.5) cDNA library constructed into pP6. Eighty-four million clones (11-fold the complexity of the library) were screened using a mating approach with Y187 (matα) and L40ΔGal4 (mata) yeast strains as described previously (Fromont-Racine et al., 1997). Eighty-five His+ colonies were selected on a medium lacking tryptophan, leucine and histidine. The prey fragments of the positive clones were amplified by PCR and sequenced at their 5′ and 3′ junctions. The resulting sequences were used to identify the corresponding interacting proteins in the GenBank database (NCBI) using a fully automated procedure. A confidence score (PBS, for Predicted Biological Score) was attributed to each interaction as previously described (Formstecher et al., 2005). The screen isolated thirty positive clones expressing six cDNA with different lengths of mouse ZSCAN21, and six positive clones with one cDNA encoding TRIM41.

Western blots

Samples were diluted in Laemmli sample buffer, incubated at 95°C for 5 min, separated by SDS-PAGE and finally transferred to Immobilon-P (Millipore) PVDF membrane. After blocking non-specific sites for 1 h at room temperature with 5% non-fat milk in Tris-buffered saline (TBS) supplemented with 0.1% Tween-20, the membrane was incubated overnight at 4°C with the indicated primary antibodies diluted in TBS-Tween supplemented with 5% milk. After washing the membranes three times in TBS-Tween, the blots were incubated with adequate horseradish peroxidase-linked secondary antibodies (Jackson ImmunoResearch Laboratories Inc.) diluted in TBS-Tween supplemented with 5% milk for 1 h at room temperature and subsequently washed three times in TBS-Tween. The immunoreactive proteins were visualized using Covalight enhanced chemiluminescent substrate (Covalab) or directly by detecting fluorescent bands using the Odyssey infrared imaging system (Li-Cor Biosciences). To confirm equal loading and transfer, the membrane was subsequently stripped and reprobed for actin or tubulin. Fiji software (Schindelin et al., 2012) was used for optical density quantitation.

GST-TRIM17 pull down assay

Mouse cerebellar granule neurons were cultured in a medium containing a low concentration of KCl for 8 hours to induce apoptosis as already described (Magiera et al., 2013), and then homogenized in lysis buffer (50 mM Tris-HCl [pH 7.5], 150 mM NaCl, 1% NP-40, 20 μM MG-132 and protease inhibitor cocktail [Sigma]). For pull down assays, the lysate was first precleared on free glutathione magnetic beads on a rotating wheel for 1 h at 4°C. Precleared lysates were then added to 1 μg of GST or GST-mouse TRIM17 recombinant proteins produced in *Escherichia coli* BL21 strain and bound to glutathione magnetic beads and rotated overnight at 4°C. Beads were washed three times with lysis buffer and once with the same buffer supplemented with 0.3 M NaCl. Materials bound to the beads were eluted by the addition of 3 × Laemmli sample buffer and incubation at 95°C for 10 min. Precipitated proteins were separated by SDS-PAGE, and analyzed by western blot using anti-mouse ZSCAN21 antibody (Millipore, catalog # AB3733, discontinued).

Transfection and culture of cells

293T, Neuro2A, U2OS and SH-SY5Y cell lines were transfected with GenJet *in vitro* transfection reagent (Ver. II) (SignaGen laboratories, Ijamsville, MD), with Lipofectamine 2000 or RNAi max (Thermofisher Scientific) according to the manufacturer's instructions. Lymphoblastoïd cell lines (LCLs) were generated by EBV (Epstein–Barr virus) transformation of peripheral blood lymphocytes collected from some of PD cohort's participants using standard methods (European Collection of Cell Cultures). Cells were maintained in RPMI medium containing 15% FBS at 37°C in 5% CO2.

Lentiviral transduction of cells

The HIV-derived lentiviral vectors pLKO.1 containing control shRNA (SHC002) (shRNA #1), the ZSCAN21 specific shRNAs TRCN0000015019 (shRNA #2) and TRCN0000015022 (shRNA #3), the TRIM17 specific shRNAs TRCN0000033825 (shRNA #4) and TRCN0000033828 (shRNA #5), and the TRIM41 specific shRNAs TRCN0000034045 (shRNA #6) and TRCN0000247961 (shRNA #7) were obtained from Sigma-Aldrich. Lentiviruses were produced as described (Swainson et al., 2008). Briefly, Lenti-X 293 T cells (Clontech) were transfected with pLKO.1 derived constructs together with the pCMVΔR8.91 and phCMV-G (expressing the vesicular stomatitis G envelope) packaging plasmids at a 3:3:1 ratio using calcium phosphate precipitation. One day after transfection, the initial culture medium was replaced by a small volume of serum-free medium for 24-30 h. The conditioned medium was harvested, passed through a 0.45 μm pore filter and concentrated by ultracentrifugation using an SW28 rotor (Beckman) at 80 000 × g for 2 h at 4°C. The lentiviruses were resuspended in serum-free medium and titrated using a p24 ELISA kit (Innotest® from Innogenetics) according to the instructions of the manufacturer. Lentiviral preparations were kept frozen in small aliquots at −80°C until use. The lentiviral preparations were added directly to the culture medium for 8 h (approximately 100 ng p24 per million) one day after cells plating. Cells were then replaced in fresh medium. SH-SY5Y cells were maintained in culture for 24 h after transduction and then selected using 2 μg/ml puromycin for additional 24 h.

Co-immunoprecipitation

Following transfection with the indicated plasmids for 24 h, cells were homogenized in lysis buffer A (50 mM Tris-HCl [pH 7.5], 150 mM NaCl and protease inhibitor cocktail) with 1% NP-40 for immunoprecipitation with anti-FlagM2 beads, and with 0.5% NP-40 for immunoprecipitation with GFP-Trap-A beads. Cell lysates were diluted 4 times in lysis buffer A without detergent and were incubated for 4 h at 4°C with anti-FlagM2 beads or GFP-Trap-A beads as indicated. The beads were then recovered by centrifugation and washed four times with lysis buffer A without detergent but supplemented with 0.5 M NaCl. Precipitates were then eluted by the addition of 3 × Laemmli sample buffer and incubation at 95°C for 5 min. Precipitated proteins were separated by SDS–PAGE and analyzed by western blot.

In situ PLA

U2OS or SH-SY5Y cells, seeded onto glass coverslips, were left untransfected (SH-SY5Y cells) or transfected with pCI-3xFlag-ZSCAN21 or untagged ZSCAN21 for 24 h alone (for U2OS cells) or together with HA-TRIM41, HA-TRIM17, HA-TRIM44, HA-TRIM5α or Flag-TRIM39 expressing plasmids (for SH-SY5Y cells). Then, cells were fixed with 4% paraformaldehyde for 20 min, washed with PBS and permeabilized with 0.2% Triton X-100 in PBS for 10 min, at room temperature. The close proximity between overexpressed Flag-ZSCAN21 and endogenous TRIM41 in U2OS cells was detected using the Duolink® *In Situ* kit (Sigma-Aldrich, Cat#DUO92004, Cat#DUO920042, Cat#DUO92014), according to the manufacturer's instructions. Briefly, cells were successively incubated with blocking solution for 30 min at 37°C, with primary antibodies against Flag (1:200) and TRIM41 (Abcam, 1:100) overnight at 4°C and with secondary antibodies conjugated with oligonucleotides (PLA probe MINUS and PLA probe PLUS) for 1 h at 37°C. The cells were then incubated with two connector oligonucleotides together with DNA ligase for 30 min at 37°C. If the two secondary antibodies are in close proximity, this step allows the connector oligonucleotides to hybridize to the PLA probes and form a circular DNA strand after ligation. Incubation, for 100 min at 37°C, with DNA polymerase consequently leads to rolling circle amplification (RCA), the products of which are detected using fluorescently-labeled complementary oligonucleotides. Cells were washed with Duolink *In Situ* wash buffers following each of these steps. In SH-SY5Y cells, the interaction between Flag-ZSCAN21 and different TRIM proteins were detected as above using primary antibodies against ZSCAN21 (Catalog # HPA023591, Sigma-Aldrich, 1:100) and HA (clone 12CA5, 1:100) or Flag (clone M2, 1:200). For untransfected SH-SY5Y cells, the interactions between endogenous TRIM41 and ZSCAN21 proteins were detected as above using primary antibodies against ZSCAN21 (Mouse, Cliniscience, 1:50) and TRIM41 (Rabbit, Abcam, 1:100). In the last wash, 1 μg/ml DAPI was added to the cells for 5 min at room temperature to stain the nuclei. Coverslips were set in Mowiol (polyvinyl alcohol 4-88, Fluka), on glass slides and analyzed by confocal fluorescence microscopy. 3D reconstitution was performed using Imaris (Bitplane) software from z series of 65 images (0,2 μm stack).

Immunofluorescence

For immunofluorescence, SH-SY5Y cells were seeded on glass coverslips, transfected as described in the figure legends, and fixed with 4% paraformaldehyde. They were then washed with PBS and permeabilized with 0.5% Triton X-100 in PBS at room temperature for 5 min. After blocking with PBS + 5% normal goat serum for 30 min at room temperature, coverslips were incubated overnight with primary antibodies (see below) diluted in PBS + 5% normal goat serum at 4°C. Cells were then washed twice in PBS and developed with Alexa Fluor® 488 and Alexa Fluor® 594-labeled goat anti-mouse and goat anti-rabbit antibodies (Molecular Probes, dilution 1:1000 in PBS + 5% normal goat serum). In the last wash, 1 μg/ml of DAPI was added to the cells for 5 min at room temperature. Coverslips were set in Mowiol (polyvinyl alcohol 4-88, Fluka) on glass slides and analyzed for fluorescence. Overexpressed Flag-ZSCAN21, Flag-ZSCAN21 p.V5I and Flag-ZSCAN21 ΔCter were detected with anti-ZSCAN21 (Catalog # HPA023591, 1:100), TRIM proteins with either anti-HA (clone 12CA5, 1:100) or anti-Flag (clone M2, 1:200) antibodies and endogenous α-synuclein using anti-α-synuclein antibody (BD, 1:50). Conventional fluorescent image acquisition and analysis were performed on work stations of the Montpellier RIO imaging facility. Intensity of α-synuclein immunofluorescence was quantified in each cell using CellProfiler software (Carpenter et al., 2006). For each image, α-synuclein intensities in individual transfected cells were compared to the average intensity of untransfected cells present in the same image, following background subtraction. Apoptosis was assessed by estimating the proportion of cells with a typical apoptotic condensed nuclei.

Ubiquitination assay

Neuro2A or 293T cells were transfected with His-ubiquitin together with the indicated plasmids. Twenty-four hours after transfection, cells were treated with 20 μM MG-132 for 6 h, before cell harvesting in PBS. Ten percent of the cell suspension were lysed in buffer A with 1% NP-40 and used as total lysates whereas the rest of the cells were lysed in 1 mL of lysis buffer B (6 M guanidinium-HCl, 0.1 M Na_2HPO_4/NaH_2PO_4, 10 mM Tris-HCl [pH 8.0]) supplemented with 0.5 M NaCl. The lysates were sonicated and cleared by centrifugation at 1,500 × g for 5 min at room temperature. Then, supernatants were supplemented with 10 mM imidazole (pH 8.0), added to 20 μL magnetic nickel beads (MagneHis Ni-Particles, Promega) and rotated for 2 h at room temperature to purify ubiquitinated proteins. Beads were washed once with lysis buffer B supplemented with 10 mM imidazole, once with 8 M urea, 0.1 M Na_2HPO_4/NaH_2PO_4, 10 mM Tris-HCl (pH 8.0) 10 mM imidazole, once with 8 M urea, 0.1 M Na_2HPO_4/NaH_2PO_4, 10 mM Tris-HCl (pH 6.3) 10 mM imidazole, 0.2% Triton X-100, 0.5 M NaCl and three times with 8 M urea, 0.1 M Na_2HPO_4/NaH_2PO_4, 10 mM Tris-HCl (pH 6.3) 10 mM imidazole, 0.2% Triton X-100. Materials bound to the beads were eluted by the addition of 3 × Laemmli sample buffer and boiling for 10 min. Then, ubiquitinated proteins and total lysate were resolved by SDS-PAGE and analyzed

by western blot using anti-ZSCAN21 antibody or against other protein of interest. When indicated, the His-ubiquitinK0 plasmid (in which all K residues have been replaced by R residues in ubiquitin) was transfected instead of the His-ubiquitin plasmid in order to detect subtle ubiquitination variations between two conditions by limiting poly-ubiquitin chains formation.

Pulse-chase experiments

SH-SY5Y cells were transfected with plasmids expressing Flag-ZSCAN21, Flag-ZSCAN21(ΔCter) or Flag-ZSCAN21 p.V5I alone or together with TRIM17-GFP, TRIM39-mCherry, HA-TRIM41 or TRIM44-mCherry expressing vectors. Eighteen hours after transfection, cells were washed twice in PBS and incubated in labeling medium (methionine and cysteine-free DMEM supplemented with 50 μM L-cysteine-HCl and GlutaMAX-I) for 1.5 h to deplete intracellular stores of methionine. Labeling medium containing 25 μCi of Easy Tag Methionine L-[^{35}S] (1175 Ci/mmol; Perkin Elmer) in 1 mL was then added for 1.5 h for metabolic labeling. Then, cells were washed three times in PBS and either harvested immediately (time 0) or washed twice and incubated for 4, 6, 8, 12 or 24 h in normal medium, before harvesting in lysis buffer A. Cell debris were removed by centrifugation and resulting supernatants were diluted seven times in buffer A without detergent. Lysates were incubated at 4°C for 4 h with anti-FlagM2 beads. Beads were recovered by centrifugation and washed four times with buffer A without detergent and containing 300 mM NaCl. Material bound to the beads was eluted by the addition of 3 × Laemmli sample buffer and boiling for 5 min. Precipitated proteins were separated by SDS–PAGE, transferred to PVDF membranes and analyzed by autoradiography. ImageJ software was used for optical density quantitation of autoradiographies.

Cycloheximide treatment

SH-SY5Y cells were transfected with indicated siRNAs. The day after, the same cells were transfected either with the same siRNAs alone (SiRNA TRIM17#1 and SiRNA TRIM41#2 for endogenous ZSCAN21) or together with Flag-ZSCAN21 for one additional day. Cells were then treated with cycloheximide (20μg/ml) for increasing times. Cell lysates were analyzed by SDS-PAGE and western-blots using anti-ZSCAN21 (1:500), anti-Flag (clone M2, 1:1000) and anti-actin antibodies (1:5000). Bands corresponding to Flag-ZSCAN21 and actin were quantified using ImageJ software. Graphs represent levels of ZSCAN21 (normalized with actin) remaining at each time point compare to ZSCAN21 level without cycloheximide treatment. Sequences of SiRNAs used:

SiRNA TRIM41#1 5′-AAGGAGACTTTCAATAGGTGT-3′
SiRNA TRIM41#2 5′-CAGACCGGCCAGAATTTAG-3′
SiRNA Control 5′-TCGAAGTATTCCGCGTACG-3′
SiRNA TRIM17#1 5′-GAACGCATTGTGCTGGAGTTTC-3′
SiRNA TRIM17#2 5′-GGTATACTGACAGATGCTT-3′

Chromatin immunoprecipitation (ChIP)

Cells were fixed by the addition of formaldehyde to a final concentration of 1% and incubated for 10 min at 37°C, before quenching by the addition of an equal volume of glycine 2.5 M for 5 min at room temperature. Cells were washed with PBS and incubated successively in wash buffer n°1 (10 mM HEPES [pH 7.3], 0.25% Triton X-100, 10 mM EDTA, 0.5 mM EGTA, protease inhibitor cocktail) and in wash buffer n°2 (10 mM HEPES [pH 7.3], 1 mM EDTA, 0.5 mM EGTA, 200 mM NaCl, protease inhibitor cocktail) for 10 min on ice. The cells were then incubated in lysis buffer (50 mM Tris-HCl [pH 7.5], 10 mM EDTA, 1% SDS, protease inhibitor cocktail). Each 200 μL aliquot of lysate was sonicated at high power for 30 min (30 s ON/30 s OFF) using a Bioruptor ultrasonicator (Diagenode). Lysates were centrifuged twice at 16,000 × g for 5 min at 4°C. The DNA content of the resulting supernatants was measured and ~100 μg chromatin was used for each immunoprecipitation. Samples were diluted 1:10 in ChIP dilution buffer (16,7 mM Tris-HCl [pH 8], 1.2 mM EDTA, 1.1% Triton X-100, 0.01% SDS, 167 mM NaCl, protease inhibitor cocktail) and were rotated overnight at 4°C in the presence of anti-FlagM2 beads. The beads were then recovered by centrifugation at 1.500 × g for 5 min at 4°C and washed successively for 10 min at 4°C with RIPA buffer (50 mM Tris-HCl [pH 8], 0.1% SDS, 0.5% sodium deoxycholate, 1% NP-40, 150 mM NaCl), high salt buffer (50 mM Tris-HCl [pH 8], 0.1% SDS, 1% NP-40, 500 mM NaCl), LiCl buffer (50 mM Tris-HCl [pH 8], 0.5% sodium deoxycholate, 1% NP-40, 250 mM LiCl) and twice with TE buffer (10 mM Tris-HCl [pH 8], 1 mM EDTA). The immune complexes were eluted by incubating the beads twice with 200 μL elution buffer (2% SDS, 100 mM $NaHCO_3$, 1 mM DTT) for 15 min at room temperature and centrifuging them at 1.500 × g for 5 min at 4°C. The supernatants were collected, supplemented with 16 μL NaCl 5 M and incubated over night at 65°C to reverse protein-DNA cross-links. An equivalent quantity of input chromatin was treated the same way. RNA and proteins were removed from the samples by the addition of 8 μL EDTA 0.5M, 16 μL Tris-HCl (pH 6.5) 1 M, 4 μL proteinase K (10 mg/ml), and 3.3 μL RNase (24 mg/ml) and incubation for 1 h at 45°C. Purified DNA from ChIP samples and input chromatin were then phenol-chloroform extracted. Purified DNA was precipitated with $NaHCO_3$ and ethanol, washed with 70% ethanol, dissolved in water and subjected to quantitative PCR as described above, using: forward primer: 5′-AG CAGAGGGACTCAGGTAAG-3′; reverse primer: 5′-GCTCCCCAAAGGGACAAGTA-3′. A standard curve of chromatin was used to quantify the results and the amount of *SNCA* promoter DNA precipitated by the antibody was expressed as the percentage of the amount of input chromatin used for each immunoprecipitation.

Oligonucleotide pull-down assay

Neuro2A cells were left untransfected and SH-SY5Y cells were transfected with the indicated plasmids for 24 h. Cells were homogenized in lysis buffer A containing 1% NP-40. Ten percent of cell lysates (Total lysate) were directly subjected to western blot or analyzed by chemoluminescence (for luciferase-fused constructs) whereas the rest (Oligonucleotide pull-down) was incubated for 4 h at 4°C with streptavidin-agarose beads (Catalog # 85881, Sigma-Aldrich) together with a duplex of biotinylated-oligonucleotides corresponding to the DNA flanking sequence of the mouse *SNCA* gene containing either the consensus binding site for ZSCAN21 or a stretch of A. A competing non-biotinylated oligonucleotide (WT oligont) was added when indicated. The beads were then recovered by centrifugation and washed four times with the lysis buffer. Precipitated proteins were either directly analyzed by chemoluminescence (using the Dual-Luciferase assay kit according to the manufacturer's instructions (Catalog # E1960, Promega) or by SDS-PAGE and western blot. Sequences for WT oligonucleotides, 5′- TAGGGAGCCGGTAAGTACCTGTAGATG-3′ /5′- CATCTACAGG TACTTACCGGCTCCCTA-3′ and negative control oligonucleotides, 5′- TAGGGAGCCGGTAAAAAACTGTAGATG −3′/5′- CATCTA CAGTTTTTTACCGGCTCCCTA-3′.

RNA preparation and RT-qPCR

Total RNA was extracted using the RNAqueous® kits (Ambion, catalog # AM1931 or AM1912, Thermofisher Scientific) and treated with DNase I from the DNA-free removal kit (Ambion, catalog # AM1906) according to manufacturer's instructions. One μg of total RNA was reverse-transcribed using 200 U reverse transcriptase Superscript II (Thermofisher Scientific, catalog # 18064014) in the presence of 2.5 μM N6 random primers and 0.5 mM dNTP. The equivalent of 6 ng of resulting cDNA was used as a template for real time PCR using a Mx3000P thermocycler (Agilent) with a home-made SYBR Green QPCR master mix (Lassot et al., 2010). PCR reactions were performed in 10 μL in the presence of 150-300 nM primers. Thermal cycling parameters were 10 min at 95°C, followed by 40 cycles of 95°C for 30 s, 64°C for 30 s and 72°C for 30 s. Data were analyzed and relative amounts of specifically amplified cDNA were calculated with MxPro software (Agilent). The human *GAPDH*, *β-2 Microglobulin* (B2M) or *hydroxymethylbilane synthase* (HMBS) amplicons were used as references. See Table S4 for the sequences of the primers used.

Subacute MPTP intoxication and RNA extraction

Mice received a single intraperitoneal injection of 1-methyl-4-phenyl-1,2,3,6-tetrahydropyridine (MPTP)-HCl or saline per day (30 mg/kg/day of free base; Sigma-Aldrich, catalog #M0896) for 5 consecutive days. Mice were euthanized at different time-points after the last MPTP injection (0, 2, 4 and 7 days for MPTP-injected mice and 7 days for saline-injected mice). N = 6-8 animals/group. Mice were euthanized by cervical dislocation, the brain quickly removed and carefully dissected and snap-frozen on dry ice. Isolation of RNA from midbrain was performed using the miRNeasy Mini Kit (QIAGEN, #T217004) following manufacturer instructions with small modifications. Tissue samples were lysed in 1 mL QIAzol Lysis Reagent and disrupted with a politron. 0.2 mL chloroform was added and samples were centrifuged for 15 min at 12,000 x g at 4°C. The aqueous supernatant was mixed with 1.5 volumes of 100% ethanol, transferred to an RNeasy Mini column and centrifuged for 15 s at 8,000 x g at room temperature. Columns were washed with 700 μl RWT Buffer and then washed twice with 500 μl RPE Buffer, with centrifugation steps in between. Elution was done in 50 μl RNase-free water and RNA preparations were quantified using NanoDrop. Quantitative RT-PCR was performed with 1 μg of RNA as described above. Data were analyzed and relative amounts of specifically amplified cDNA were calculated with MxPro software (Agilent). The mouse *β2 Microglobulin* (B2M) amplicons were used as references. See Table S4 for the sequences of the primers used.

In vitro ubiquitination

HA-TRIM41 and HA-TRIM41 p.R534C were first transcribed and translated *in vitro*. For this, 2 μg of the different plasmid constructs were incubated for 2 h at 30°C in 50 μL of the TNT® SP6 coupled wheat germ extract system (Promega, catalog # L5030), according to the instructions of the manufacturer. Five μl of the *in vitro* translation reaction were incubated for 120 min at 37°C in the presence of 50 ng of human recombinant His-tagged ubiquitin-activating enzyme E1 (from BostonBiochem, catalog # E-304), 10 μg of ubiquitin (Nterminal-Histidine tagged, Sigma-Aldrich, catalog # U5507) and in the presence, or not, of 500 ng human recombinant His-tagged ubiquitin-conjugating enzyme (E2) Ube2d3 (from BIOMOL International, catalog #U0880) in 20 μL (final volume) of ubiquitination assay buffer (50 mM Tris-HCl pH7.5, 50 mM NaCl, 4 mM ATP, 4 mM $MgCl_2$, 2 mM DTT, 10 mM phosphocreatine, 0.5 U creatine kinase, 20 μM $ZnCl_2$). For TRIM17 inhibition, recombinant GST-TRIM17 or GST alone were added to the reaction. Reaction products were separated by SDS-PAGE, transferred to PVDF membranes and analyzed by western blot using anti-Flag and anti-GST antibodies.

Sanger sequencing

In all 190 index cases and 190 control subjects, the seven, four, and six coding exons and intron-exon boundaries of *TRIM17* (GenBank: NM_016102), *ZSCAN21* (GenBank: NM_145914) and *TRIM41* (GenBank: NM_033549), genes respectively were PCR-amplified using selected primers and sequenced bi-directionally using the Big Dye Terminator Cycle Sequencing Ready Reaction kit, on an ABI 3730 automated sequencer, and SeqScape v2.6 analysis software (Applied Biosystems). Mutation nomenclature follows HGVS recommendations with +1 as A of ATG initiation codon (Ensembl: ENST00000366698 transcript for *TRIM17*, ENST00000292450 transcript for *ZSCAN21*, ENST00000315073 transcript for *TRIM41*). Nucleotides frequencies in Table S2 were

from ExAC and 1000 genomes (Abecasis et al., 2012) databases. The pathogenicity of novel missense variants was predicted using CADD prediction (https://cadd.gs.washington.edu/) (Kircher et al., 2014) and PolyPhen2 (http://genetics.bwh.harvard.edu) (Adzhubei et al., 2010) softwares. The ClustalW program on the European Bioinformatics Institute server (https://www.ebi.ac.uk/clustalw/) (Sievers et al., 2011) was used to align the human TRIM17 and ZSCAN21 proteins and their closest homologs. See Table S4 for primers used for PCR and sequences.

QUANTIFICATION AND STATISTICAL ANALYSIS

Unless specifically specified in figure legends, all data are the mean ± SEM of at least three independent experiments, one-way ANOVA (for column graphs) or two-way ANOVA (for kinetics experiments) followed by Dunnett's multiple comparison test were performed using GraphPad Prism 7.00 for Mac OS X (GraphPad Software, La Jolla California USA).